7-1-2016

# Damping and Mechanical Behavior of Multiwalled Carbon Nanotube Epoxy Composites

Rochelle Piatt

Rochelle Piatt

*Candidate*

Mechanical Engineering

*Department*

This thesis is approved, and it is acceptable in quality and form for publication:

*Approved by the Thesis Committee:*

Dr. Mehran Tehrani , Chairperson

Dr. Yu-Lin Shen

Dr. Mahmoud Reda Taha

# DAMPING AND MECHANICAL BEHAVIOR OF MULTIWALLED CARBON NANOTUBE EPOXY NANOCOMPOSITES

**by**

**ROCHELLE PIATT**

**UNIVERSITY OF NEW MEXICO**
**B.S.M.E**
**MAY 2014**

**THESIS**

**Submitted in Partial Fulfillment of the**

**Requirements for the Degree of**

**Master of Science**
**Mechanical Engineering**

**The University of New Mexico**

**Albuquerque, New Mexico**

**June 2016**

# DEDICATION

I would like to dedicate this thesis to those who have stood by and believed in my potential throughout this entire process.

To my parents, who have always been there to support and encourage me and listen to all of my long, and sometimes boring, explanations about my research. Thank you for the constant encouragement and guidance and for being my first teachers on this journey of learning. You opened my eyes to always wanting to know more and being interested in everything.

I would also like to dedicate this thesis, in loving memory, to the person who gave me the confidence in a subject I had already determined I wasn't good enough to conquer. Natalie Whitezell believed in my ability and potential to grow in engineering. She helped me to find my confidence in math again and encouraged me to continue in a field that had a heavy math presence. I would not have considered engineering as a career choice without her constant help and encouragement to get out of my comfort zone. She went above and beyond the duties of a teacher and became my mentor and advisor. So, to my personal cheerleader, who I know will always be that little voice in my head telling me that I can do it, thank you.

# ACKNOWLEDGMENTS

I would like to thank Dr. Mehran Tehrani, my advisor and chair of my thesis committee. His guidance and encouragement during the last two years of research and study has helped me to continue pursing my learning goals. His lessons and shared knowledge will continue to help me as I continue in my career.

I would also like to thank those who have helped me with my research and lab work during these past couple of years. The ASEM Lab Group, where I did my thesis work the past two years helped me with various equipment set-ups gave me valuable insight. I would like to also thank one of the ASEM Lab Group members, Nekoda van de Werken for working with me on different dispersion methods and performing all of the SEM work for my thesis.

# DAMPING AND MECHANICAL BEHAVIOR OF MULTIWALLED CARBON NANOTUBE EPOXY COMPOSITES

**by**

**Rochelle Piatt**

**B.S. Mechanical Engineering, University of New Mexico, 2014**

**M.S. Mechanical Engineering, University of New Mexico, 2016**

## ABSTRACT

Polymeric materials exhibit a viscoelastic (time-dependent) behavior, which is characterized using creep, stress-relaxation, and dynamic mechanical analysis (DMA) tests at different temperatures. Nanoindentation techniques are non-destructive and only require a small sample to perform experiments. While instrumented indentation has enabled high-throughput measurement of many mechanical properties for bulk and thin-film polymer samples such as elastic modulus, hardness, and creep compliance, there is no available technique to accurately extract the temperature-dependent viscoelastic properties using nanoindentation. On the macro-scale, DMA can measure damping factor ($\tan\delta$) for viscoelastic solids and glass transition temperature ($T_g$) can be readily determined from temperature-dependent $\tan\delta$ measurements. This thesis attempts to find correlations between nanoindentation creep and impact tests to the macroscale viscoelastic properties measured via DMA. For this purpose, epoxy nanocomposites with different types and loadings of multiwalled carbon nanotubes (MWCNTs) were fabricated and characterized.

Scanning electron microscopy (SEM), thermogravimetric analysis (TGA), differential scanning calorimetry (DSC), and Raman spectroscopy were used to assess carbon nanotube quality, dispersion state, and epoxy curing. Modulus, hardness, and strain rate sensitivity were measured at elevated temperatures using nanoindentation and compared to DMA results.

# TABLE OF CONTENTS

# LIST OF FIGURES

**1**

# LIST OF TABLES



**2**

# Chapter 1: Introduction

## 1.1 Motivation

Dynamic mechanical analysis (DMA) is the conventional technique to characterize the viscoelastic properties of materials. In DMA, a sinusoidal stress (strain) is applied to the sample while the output strain (stress) is measured. There is a phase lag between the stress and strain due to the materials viscous nature. Tangent of this phase lag angle is defined as the material's damping.

The $T_g$ of a polymer is the temperature at which it goes from a hard, glass-like state to a softer and more viscous state. Polymers are used at temperatures above or below their glass transition temperatures to take advantage of certain properties. Accurate measurement of the $T_g$ of polymer-based systems is crucial in that the operation temperature of such materials must be maintained in accordance to their $T_g$. DMA can readily measure this temperature by identifying the temperature at which the damping ($\tan\delta$) has a maximum.

Nanoindentation techniques are non-destructive and only require a small sample to perform experiments. While instrumented indentation has enabled high-throughput measurement of many mechanical properties for bulk and thin-film polymer samples such as elastic modulus, hardness, and creep compliance, there is no available technique to accurately extract the temperature-dependent viscoelastic properties using nanoindentation. Many researchers have worked to find correlations between the DMA and nanoindentation tests due to the advantage of a smaller sample size needed for nanoindentation testing. Nano-DMA, as an analogous test method to macro-scale DMA, was introduced in many instrumented indentation systems. This module works on the same basis as macro-DMA, where the application of a

sinusoidal load induces a phase-shifted sinusoidal indentation depth response. Nano-DMA has, however, found little success to either reproduce or accurately measure viscoelastic properties of polymers due to its complex measurement nature, non-linearity, and high noise levels in the phase lag measurements.

Analysis of nanoindentation creep tests (nano-creep) was introduced to determine tanδ from nanoindentation tests.[1-3] Nanocreep involves recording the depth while maintaining a constant nanoindentation load. The phenomenological method of determining tan $\delta$ is based on quasi-static nanocreep tests and, therefore, may not be a reliable and accurate way of measuring tan $\delta$, which is a dynamic property. Moreover, while stresses in DMA tests are limited to linear viscoelastic regime, nanocreep test is usually conducted under nonlinear viscoelastic or viscoplastic regime. Using spherical tips instead of sharp Berkovich tips may alleviate this issue.

On the contrary, nano-impact test (the decaying response of an energized indenter impact on the sample) can be used to extract viscoelastic properties of polymers. This test, similar to DMA, is dynamic and does not require any specific calibration.

This thesis attempts to find correlations between nanoindentation creep and impact tests measured using a spherical tip to the macroscale viscoelastic properties measured via DMA. Epoxy nanocomposites were chosen for this purpose due to their distinct viscoelastic behavior and $T_g$. Both DMA and nanoindentation techniques were utilized to characterize the mechanical and viscoelastic properties of polymeric and carbon nanotube (CNT) epoxy nanocomposite systems at elevated temperatures. For this purpose of thesis, well-dispersed nanocomposites were fabricated.

## 1.2 Materials and Processing

### 1.2.1 Carbon nanotubes

Carbon nanotubes (CNTs) were first discovered by Iijima in 1991 [4] and have since been widely researched. The structure of a CNT can be visualized by rolling a Graphene sheet (carbon atoms in a planar honeycomb arrangement), the properties of which are determined by their size, chirality (rolling angle), and whether they contain single or multiple shell(s). The singular rolled tube is known as a single walled carbon nanotube (SWCNT) and multiple rolled tubes within one another make up a multi-walled carbon nanotube (MWCNT).

The general geometry and structure of CNTs can be visually characterized using a variety of methods. Among the most common are Transmission Electron Microscopy (TEM) and Scanning Electron Microscopy (SEM).

Carbon nanotubes experience van der Waals forces that hold nanotubes together, but also cause the formation of nanotube bundles [5]. These bundles form aggregates, which could be detrimental to the properties of the matrix they are used in. Such aggregates are formed during CNT synthesis and entrap catalyst particles that are used for CNT growth. Carbon nanotubes also contain defects in their crystalline structure. In order to assure that the CNTs being used in this study were as pure and free from defects as possible, graphitized CNTs were utilized. Graphitization of CNTs is the high temperature annealing of CNTs to remove defects and impurities [6].

Two of the most important factors in achieving the desired properties in CNT composites are good dispersion and bonding between the CNTs and polymer [7]. The dispersion and bonding in CNT nanocomposites can be achieved by a variety of chemical and mechanical methods.

### 1.2.2 Chemical Dispersion

Chemical dispersion can be achieved with the help of CNT surface modifiers (surfactants). Carbon nanotubes have a smooth and non-reactive surface that does not interact with most solvents. Surfactants are amphiphilic molecules that can aid the dispersion of CNTs in various solutions. They have a hydrophilic polar head group and a hydrophobic tail group. The type of surfactant (cationic, anionic, nonionic, zwitterionic) is based on the head group charge [8]. For example, Triton X-100 (which has many chemical names including *t*-Octylphenoxypolyethoxyethanol) is a non-ionic surfactant used for the dispersion of CNTs in aqueous solutions and can potentially enhance the bonding of CNTs to epoxy matrices[9, 10]. The surfactant forms a weak bond to the outer surface of CNTs and allows for the dispersion of CNTs and separation of bundles into individual CNTs. Figure 1 depicts how a surfactant attaches to the outer walls of the CNTs.

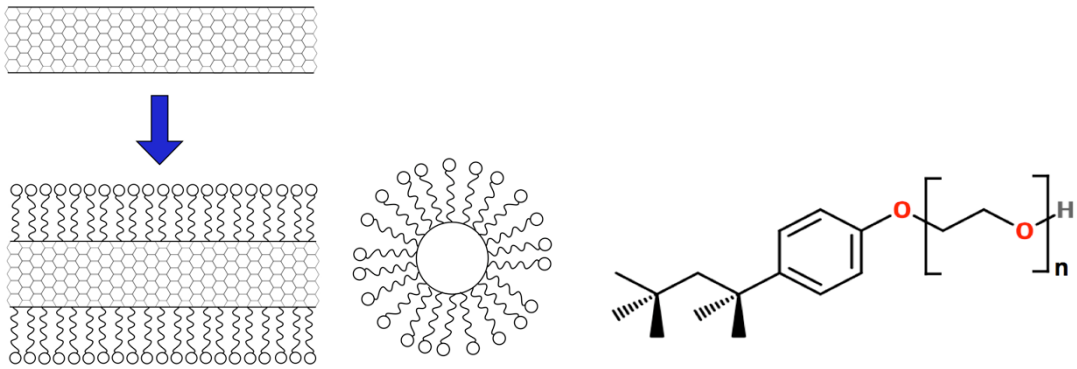


**Figure 1: Left to Right - Surfactant on the walls of a CNT (side view); Surfactant on walls of a CNT (cross section view); Triton X-100 molecular formula**

The right amount of surfactant is needed to get the best dispersion. This amount is called the critical micelle concentration (CMC). Micelles are the self-organization of the surfactant molecules into small bundles. The CMC is the point at which the surfactant can adequately coat the tubes to disperse the bundles into individuals without forming micelles in the solution. An amount less than the CMC will not result

in a good dispersion and leave bundles in solution. Concentrations higher than the CMC will cause more bundles to form in the dispersion.[10]

Another surface modification of CNTs is known as the functionalization. There are different types of functionalization including defect, covalent, and non-covalent functionalization [11]. Carboxyl functionalized MWCNTs were used in this thesis. CNTs are oxidized to remove impurities, which in return leaves defects on the tubes in the form of -COOH groups [11]. Carboxyl groups alleviate van der Walls attraction between CNTs that cause bundling and can form covalent bonds to epoxy matrices.

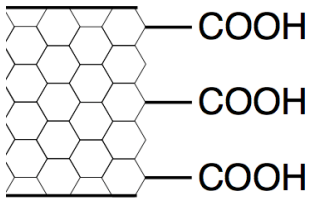


**Figure 2: Depiction of -COOH groups on the tube ends of a CNT**

The carboxyl groups that form on the CNTs are most commonly on the open ends, more so than the outer walls, due to the higher concentration of defects on the ends. These defects make for a better reactivity with the oxidation process. [5]

While the functionalization of the CNTs can improve bonding of the CNTs with the epoxy matrix, it is unclear if that bonding will cause issues with the final curing of the nanocomposite and resulting mechanical and viscoelastic properties.

### 1.2.3 Mechanical Dispersion

Mechanical dispersion includes a variety of methods including bath sonication, tip sonication, shear mixing, ball milling, and many others[12-14]. The methods utilized in this thesis includes shear mixing, tip sonication, and centrifugation.

Shear mixing draws the solution into a mixing head and pushes the solution through a narrow space between rotor and stator walls, shearing CNTs into uniform particles. The shear mixing does not damage CNTs, but will only break their agglomerates down into a uniform size. Once these agglomerates are broken down, the shear mixing process cannot aid in further dispersion and individualization of nanotubes. Product of shear mixing contains bundles of CNTs that can be hundreds to thousands of entangled CNTs.

Ultrasonication is needed to complete the dispersion of CNTs in solution. Tip sonication allows for a more focused and direct form of sonication. The tip sonicator has three major parts namely generator, converter, and probe/horn. Tip sonication is a direct form of sonication, where the probe is inserted directly into the solution. The probe vibrates while the tip expands and contracts during operation. The amount of expansion and contraction of the tip is the amplitude of sonication. [15] This process creates the cavitation that is indicative of the sonication process. The cavitation bubbles creates a high-energy stress wave upon bursting that break down and unzips nanotubes from their bundles. When dispersed, nanotubes can re-bundle if not stabilized.


**Figure 3: Tip sonication system**

Bath sonication is more of an indirect form of sonication where the sample is placed inside a water bath. The outer walls of the water bath cover a generator that causes the sonication energy. Bath sonication is less powerful than tip sonication but is a technique that can process larger sample sizes and is less likely to damage nanotubes. Bath sonication, will not produce the best CNT dispersion possible. The sonication energy is strong enough to break up some CNT bundles, but not enough to fully individualize them (unless over extended periods of time and for very dilute CNT solutions). However, it can prevent separated nanotubes from re-agglomerating while causing minimal damage to the CNTs.

Both types of sonication cause damage to CNTs. Studies have shown that longer sonication times are beneficial to dispersion[16]. Intense sonication, however, causes too much damage and leaves CNTs unusable. A characterization step is required to check CNT dispersion in solution and ensure that they are not damaged. More information is provided in 2.3.1Raman Spectroscopy.

## 1.3 Nanocomposites

Nanocomposites processed and tested in this thesis are known as two-phase composites. Two-phase nanocomposites usually consist of a nano-reinforcement phase (CNTs in this case) and a matrix (epoxy in this case). There are also multiple-phase composites, which can include a third addition for reinforcements. Many researchers have, for example, looked into three phase composites that consist of carbon fibers and epoxy, with CNTs to reinforce the matrix.[7, 10, 17-19]

Mechanical and viscoelastic properties of polymers are very desirable for many applications. The addition of CNTs can enhance many of these properties. This enhancement usually depends on the degree of dispersion, CNT-epoxy bonding and processes used for dispersion.

Because of the many different ways researchers are dispersing CNTs into polymer matrices, there have been varying and, sometimes conflicting, studies in mechanical and viscoelastic properties of the resulting nanocomposites. Researchers have used various solvents, surfactants, mechanical dispersion methods, and processes to disperse CNTs. One such variation is the dispersion of CNTs in a resin, a resin/solvent solution, hardener, or directly into the mixed resin/hardener mixture [20]. Variations on top of that are whether or not CNTs are chemically modified during or before the dispersion process as well as the type of CNTs used [21-24]. Moreover, depending on their synthesis method, CNTs can have different properties. Therefore, the best dispersion processes are the ones that achieve the best properties of the nanocomposites

## 1.4 Test Methods

### 1.4.1 Nanoindentation

Instrumented nanoindentation can be used to evaluate various material parameters using the collected data from load and depth of indentations on material surface. One of the most popular methods for analyzing nanoindentation load-depth data to extract elastic modulus and hardness values is the Oliver and Pharr method [25, 26]. The depth-load data plot from a single indentation can give a lot of insight about the tested material properties.

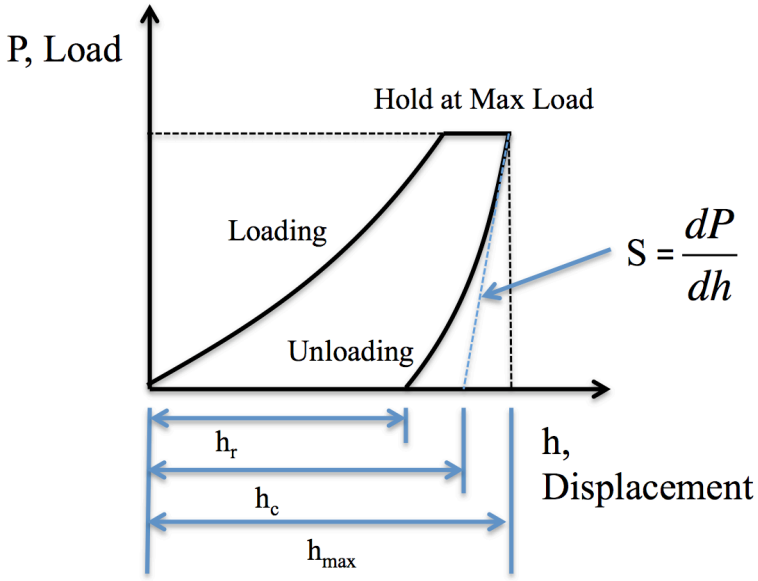


**Figure 4: Typical load vs. displacement nanoindentation data**

The plot in Figure 4 is a representative nanoindentation load-depth plot. There is a loading period, a dwell period at the maximum load, an unloading period and sometimes a dwell for thermal drift correction. Dwell at maximum load is intended to eliminate any viscoelastic response upon unloading. Constant force data (creep data) can be also analyzed to acquire viscoelastic properties.[1] Many authors have explored and compared nano/micro- to macro-scale techniques for measuring

viscoelastic properties of materials[2, 3, 27-32]. The slope of the unloading curve can be correlated to stiffness of the material following Oliver and Pharr analysis:[25, 26]

$$E_r = \frac{1}{2}\frac{\sqrt{\pi}}{\sqrt{A}}S \qquad (1)$$

Where, S is slope of the unloading curve, A is contact area and $E_r$ is the reduced modulus of the material. There are different methods that correlate indentation depth to contact area, A. As shown in the example plot of Figure 4 and Figure 5, different depths can be used for this purpose; $h_r$, $h_c$, and $h_{max}$, refer to the depth of the remaining impression in the sample, the depth of the contact circle, and the depth beneath the free surface, respectively. Usually contact area is calibrated as a function of indentation depth by performing nanoindentations at different depths on a material of known properties and back calculating the contact area. The indentation profile of a spherical indenter, like the one used in the nanoindentation characterization, is shown in Figure 5. The spherical indenter, in this case, was used because it can be used to study the plastic-elastic transition.[33]

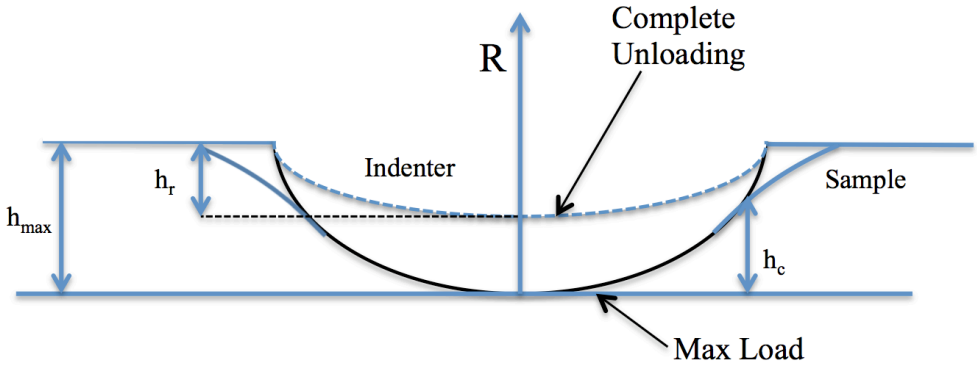


**Figure 5: Sample indentation of spherical indenter tip**

The Elastic modulus of the material can be calculated using the following:

$$\frac{1}{E_r} = \frac{(1-v_s^2)}{E_s} + \frac{(1-v_i^2)}{E_i} \qquad (2)$$

The indenter properties needed for this formula are the modulus, $E_i$, and Poisson's ratio, $\nu_i$. The spherical indenter was made out of diamond, and the material properties can be found. $E_s$ and $\nu_s$ correspond to the sample's elastic modulus and Poisson's ratio. For polymeric samples, the second term in the above formula is very small compared to the first one and can be neglected. Poisson's ratio for all of our samples is very similar. We therefore report the $E_r$ values here instead of the $E_s$.

We adopted the analysis of Gray et al. [3] to extract viscoelastic properties from the nanoindentation creep data. The creep data is collected from the dwell period at the maximum load during an indentation test. This particular analysis uses the indentation creep data to get an exact fit using the following equation.

$$D(t) - D(0) = A\ln(Bt + 1) \qquad (3)$$

*D(t)* is the indentation depth during the dwell period, *D(0)* is the depth at the onset of creep, and *t* is the time. The NanoTest 600 program then uses the best fit to the data to extract the constants A and B. The strain rate sensitivity parameter, *A/d(0)*, can then be calculated. The strain rate sensitivity parameter is the ratio between the time dependent deformation and the deformation encountered while initially loading the sample.[1] Gray et al [3] studied correlations between the strain rate sensitivity from nanoindentation tests and tanδ from DMA tests for various polymers, both at room temperature and elevated temperatures. They concluded that there is a correlation between the strain rate sensitivity and the tan delta at room temperature and that the high strain rate sensitivity values and low B values were only observed in the vicinity of glass transition temperature[3]. The correlation of strain rate sensitivity parameter and tanδ, observed by Gray et al. [3] were determined to be linear. It has also been concluded that the strain rate sensitivity parameter is an efficient way to look at glass

transition temperature deformation during elevated temperature testing[1]. Therefore, the strain rate sensitivity for nanocomposites would be compared later in this thesis to the tanδ measurements extracted from the DMA method, Chapter 5: Correlation of DMA and Nanoindentation.

Nano-impact testing can also be used to extract viscoelastic properties. In this method of testing, the indenter is backed away from the sample and then accelerated towards it. The indenter impacts the sample and the depth-time data is collected. The oscillations collected from the impact and subsequent "bouncing" of the indenter against the sample can be used as a visual or if analyzed as quantitative comparison of dynamic damping.

### 1.4.2 The NanoTest System

A Nano Test 600 was used in this study. A full background of the particular system, set up, and calibration is detailed in the following section. The Nano Test 600 is a pendulum based nanoindentation machine developed by Micro Materials Ltd. United Kingdom.

The system is placed inside a thermally insulated cabinet. This cabinet serves to reduce air turbulence that would upset the pendulum and provides a thermally controlled environment.

At the heart of the NanoTest system is a pendulum that can rotate on a frictionless pivot, Figure 6. A coil is mounted at the top of the pendulum; with a coil current present, the coil is attracted towards a permanent magnet, producing motion of the diamond tip towards the sample and into the sample surface. The displacement of the diamond tip is measured by means of a parallel plate capacitor. One plate of which is attached to the diamond holder. When the diamond moves, the capacitance changes,

and this is measured by means of a capacitance bridge.

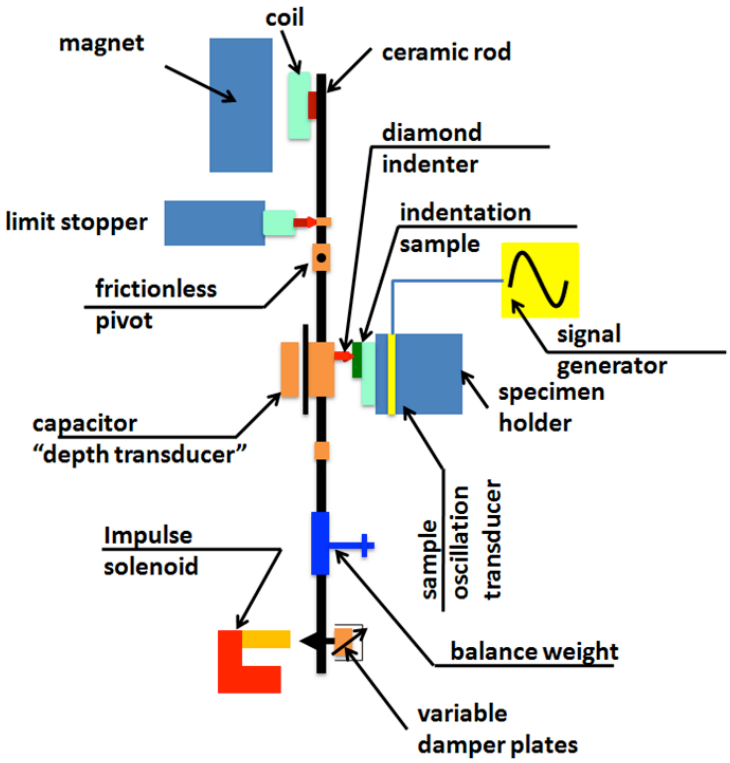


**Figure 6: Schematic of the NanoTest 600**

### 1.4.3 Elevated Temperature Testing

The NanoTest system can perform nanoindentation and impact testing at elevated temperatures. The only difference between the original setup and thermal testing setup are the additions of the indenter/heat shield and the heated sample stage block. The image in Figure 7 shows the setup of the NanoTest system for elevated temperatures.

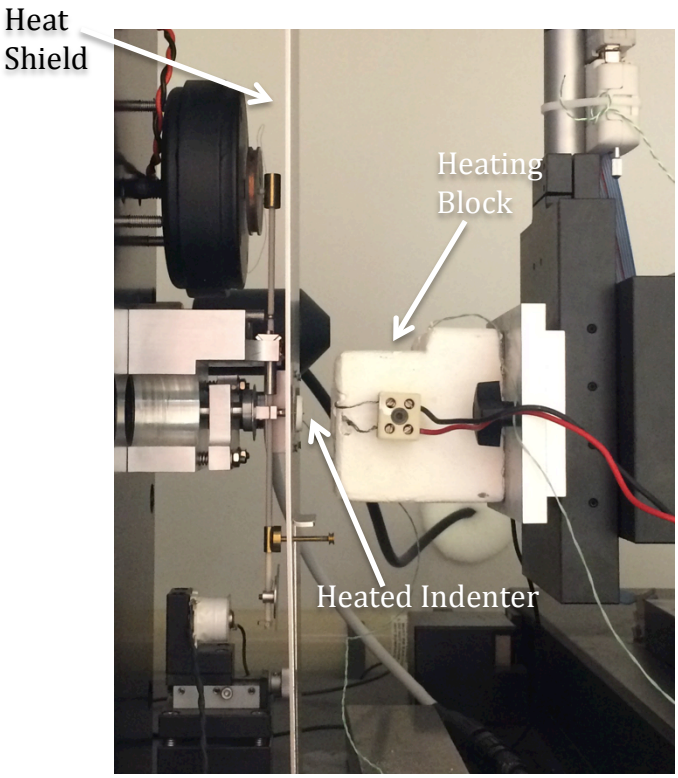


**Figure 7: NanoTest system setup for thermal testing**

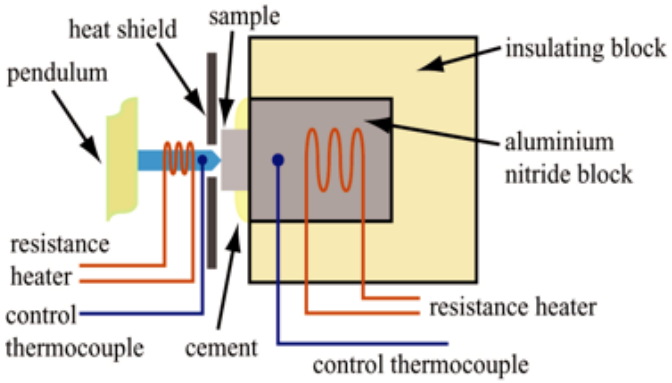


**Figure 8: Schematic of the heating block used for thermal testing. Reproduced from M. Tehrani [34]**

The samples are attached to the heating block using thermal cement. This ensures uniform heating throughout the sample and its surface. The sample holder block can be heated separately from the indenter tip. The indenter tip is attached to a heat shield. The heat shield is to keep any heat from affecting the rest of the system. Thermocouples were placed on both the indenter tip and the sample heating block to determine actual temperatures vs. temperature readout during a heating cycle. This

data was used during the current experimentation to determine what temperatures the indenter tip and sample hot stage should be set to.

## 1.5 Dynamic Mechanical Analysis

### 1.5.1 Viscoelasticity

Elastic materials store all of the energy from the loads applied to them and will return to their original shape when the load is removed. A viscous liquid has no defined shape and will continue to deform under load. Viscoelasticity is the combination of properties for an elastic solid and viscous liquid. When undergoing deformation, a material may exhibit viscoelastic characteristics. The viscoelasticity of a material is observed through both viscous and elastic responses to deformation. Viscoelastic materials are very useful for the applications of damping and shock absorption. Viscoelastic materials exhibit time dependent stress and strain. Two of the main characteristics observed with viscoelastic materials are creep and stress relaxation. In the case of viscoelastic creep, strain can increase over time with a constant stress. A viscoelastic material will return to its original shape after the stress has been removed but will retain a memory of the stress applied for an amount of time. If the material is held at constant strain and elevated temperature, the stress will begin to decrease. This phenomenon is known as stress relaxation.

Viscoelasticity can be measured in two different ways; transient and dynamic. Most viscoelastic characterization techniques are transient and include creep and stress relaxation comparisons[35]. Dynamic viscoelastic characterization includes the application of a stress or strain cyclically over time; DMA. DMA is most commonly used to characterize the thermo-mechanical response of polymeric samples.

The moduli that are calculated from DMA are referred to as the Storage Modulus and Loss Modulus. The ratio of the loss modulus to the storage modulus is known as the tanδ. The tanδ, refers to the damping ability of the material and is simply the tangent of phase lag angel between stress and strain. Storage and loss moduli are the ratio of stress amplitude to strain amplitude multiplied by cosδ and sinδ, respectively. The peak of the tanδ curve will also be used to measure the glass transition temperature.

### 1.5.2 Viscoelastic Measurements from Instrumented Indentation

There are many different methods to study the mechanical and viscoelastic properties of nanocomposites, with some being at the macro- level and others being at the nano- level of characterization. Differing results by various research groups have resulted in differing opinions on the correlation of macro- and nano- characterization methods. This thesis was put together to explore the relationship between two different methods. DMA uses larger sample sizes that are manipulated using clamps and forces to characterize the various properties. Nanoindentation is method that uses a much smaller sample to measure viscoelastic properties of materials. A very small indenter is used to apply a force and measure the material response during loading, unloading, and using impact. Because of the very small area of sample that is needed to perform nanoindentation tests, this method will be the nano- testing performed on the CNT nanocomposite samples.

The DMA test method setup uses a strain rate and constant frequency, during a temperature ramp, to measure the viscoelastic response at high temperatures. The nanoindentation test method will also be tested at similar temperature to those of the DMA to get a comparison. The glass transition temperature, by method of tanδ measurements, and the storage modulus from both test methods will be used as the comparison between the two methods.

To achieve the goal of the test comparisons, reproducible nanocomposite had to be fabricated. There are many different ways to make CNT nanocomposites, and many different types of CNTs that can be used. Every dispersion process and all of the materials that can be used will ultimately play a factor in the final properties of the produced nanocomposite. The processing methods described in this thesis were decided based upon best dispersion method, and not necessarily best measured properties.

# Chapter 2: Nanocomposite Characterization and Processing

## 2.1 Materials

Two different types of CNTs were utilized in the following experimentation. All CNTs were graphitized to a 99.9% purity and COOH-functionalized. The graphitization removes all amorphous carbon and catalysts, leaving the CNTs with a 99.9% purity. The defect functionalization is then performed, most likely using mixtures of nitric and sulfuric acids. MWCNTs were purchased from Nanostructured & Amorphous Materials Inc. (NanoAmor). The aspect ratio of carbon nanotubes have been shown to play a role in the mechanical properties of nanocomposites[36]. Two aspect ratios of CNTs were tested to determine which CNTs gave the higher improvement of properties.

| Referred to as | Length | Outer Diameter | Inner Diameter | Aspect Ratio |
|---|---|---|---|---|
| Long | ~50 μm | 8-15 nm | 3-5 nm | ~5000 |
| Short | 10-20 μm | 50-80 nm | 5-15 nm | ~300 |

**Table 1: Dimensions of graphitized COOH-MWCNTs from NanoAmor.**

Experimentation using different aspect ratios of CNTs and at different concentrations in the nanocomposite, was used to determine the most repeatable and greater increase in all measured properties. The final samples, representing the most repeatable results and increase in properties, were then utilized in the final mechanical tests.

The COOH-functionalization was desired to improve the covalent bonding of the CNTs with the epoxide groups in the polymer matrix. This bonding improves stress

transfer from the matric to CNTs, when the nanocomposite is subjected to mechanical loads.

The graphitization removes all amorphous carbon and catalysts, leaving the CNTs with a 99.9% purity. The defect functionalization is then performed. The only defects that should be seen in the CNTs are the COOH- functional groups used for bonding.

The aspect ratio of carbon nanotubes (the ratio of length to diameter) have been shown to play a role in the mechanical properties of nanocomposites [36]. The aspect ratios of the CNTs are listed in **Error! Reference source not found.**. Two aspect ratios of CNTs were tested to determine which CNTs gave the higher improvement of properties. Those samples were then used to compare the nano- and macro- test methods of nanoindentation and DMA. Some studies have determined that CNTs with a higher aspect ratio can lead to an increase in the Young's Modulus of a CNT nanocomposite. [36] It is unclear how this would affect the dispersion of the CNTs in epoxy, the cure rate of the epoxy, and the bonding of the CNTs with the epoxy. For the same dispersion, CNT-polymer interfacial bonding, and identical quality CNTs, higher aspect ratio CNTs are supposed to be more effective in improving properties of polymer. The CNTs are COOH- functionalized at different aspect ratios, which could cause significant differences in processing and result in different mechanical properties than expected.

Different solvents were tested for CNT dispersion and compatibility with the epoxy. Ethanol, acetone, tetrahydrofuran (THF), and dichloromethane (DCM) were among the solvents tested for dispersion and effect on the two epoxies tested. The main concerns were CNT dispersion in solvent, yield after centrifugation, CNT dispersion in the epoxy, and effect of the solvent on epoxy curing and properties. There were two

different epoxies that were tested with the solvents to determine which would be better for the final application.

EPON 815C resin with Epikure 3282 hardener was the first epoxy choice. EPON 815C is a low viscosity bisphenol A based resin. The low viscosity of the resin is what made it appealing for the process of making samples. The addition of CNTs to the resin makes it very viscous and more difficult for further processing. Epikure 3282 is a hardener made from a modified aliphatic amine adduct. The hardener is used in cases where a fast cure rate at room temperature is needed. The recommended EPON:Epikure mix ratio is 100:20 parts by weight.

Aeropoxy PR2032 is a medium viscosity resin containing a diphenylolpropane (bisphenol A) and a multifunctional acrylate. The hardener used was Aeropoxy PH3670, which has a pot life of four hours and will cure with the resin fully at room temperature, but takes an extended amount of time. The recommended mix ratio of Aeropoxy resin to hardener is 100:27 by weight. Aeropoxy properties are listed in Table 2.

| | PR2032 with PH3670 | ASTM Method |
|---|---|---|
| Mix Ratio | 100:27 By Weight or 3 to 1 By Volume | PTM&W |
| Pot Life | 4 Hours | D2471 |
| Tensile Modulus, GPa | 17.58 | D638 |
| Flexural Modulus, GPa | 17.31 | D790 |
| Glass Transition Temperature | 97.78 C | TMA |
| *Modulus values were derived with A 10 Ply Laminate, Hand Lay-up, Style 181 Glass Fabric, 55% Glass Content | | |

**Table 2: Mechanical properties of Aeropoxy PR2032 and PH3670. (PTM&W)**

### 2.2 Sample Processing

A master solution will be made with the desired amount of solvent and CNTs. CNTs will be mixed with the solvent at a 1:1 mg/ml ratio. The mixture was stirred using an

IKA shear mixer at the 25000 rpm for a total of 5 minutes and further dispersed using tip sonication in an ice bath (2 seconds on, 2 seconds off) for a total energy of 0.5kJ/mg of CNTs at 44% amplitude. The high-energy intensity of the tip sonication increases the temperature of the solution and can evaporate of the solvent. Therefore, an ice bath is needed during the tip sonication processing. The shear mixer breaks up large bundles of the CNTs. It is only effective until the CNTs are broken down into a micron-sized regime, then tip sonication needs to be used for further de-bundling and dispersion. This break down and separation is important for the surfactant to bind to the outer walls of the tubes and allows the particles to uniformly disperse throughout the solvent. The quality of CNT dispersion in the solution can be tested by adding a droplet of the solution to a clean beaker with new solvent. If the CNTs are well dispersed in the solution, the solution should spread evenly in the unmixed solvent and no CNT aggregates will be observed.

The CNT/solvent solution will be centrifuged at 2000 rpm for 10 minutes. The supernatant will be decanted and will contain evenly dispersed CNTs while the bottom contains bundled CNTs that were not dispersed. To determine how much of the original amount of CNTs were successfully dispersed, the bottom part of the centrifuged solution will be collected and allowed to dry out in the oven. The resulting residue will be weighed to determine the amount of CNTs in the top solution.

The final yield of CNTs that are uniformly dispersed will be used to determine the amount of solution needed to achieve the desired CNT weight for the composite samples.

A drop of the uniformly dispersed and separated solution can be dried on a glass slide and used for the final Raman test. If those CNTs are proven to be relatively undamaged, the solution can be used in the epoxy samples.

There were two concentrations of CNT nanocomposites fabricated. The CNT dispersion and their effects on the overall properties of the tested samples determined the two concentrations. The 1wt% concentration is enough to get good mechanical property enhancements, while still being easy to disperse evenly in the matrix. Anything over 1wt% increases the amount of CNT agglomerations. Any concentration below 0.3wt% would have too minimal effects on the properties of the nanocomposites. Therefore, it was determined that the two concentrations would be 0.3wt% and 1wt% CNTs in epoxy.

The epoxy resin will be mixed at a 100:27 weight ratio to the hardener. The resin is Aeropoxy PR2032 and the hardener is Aeropoxy PH3670. This amount of epoxy will fill up about 2 cuvette tubes and make multiple test samples.

The following table shows the calculated amount of CNTs needed to get the correct loading (weight%) per sample. The yield of CNTs uniformly dispersed and the amount of CNT per volume of solution will be used to determine the correct amount of CNT solution to add to each sample.

CNT solutions for the 0.3wt% and reference samples will be diluted with DCM so that the volume of all solutions is equivalent to that of the 1wt% sample. This amount will be different for every master solution and based off of the amount of unbound CNTs collected.

The CNT solution will be added to the resin. The resin solution is mixed using a solvent removal system, custom built for this procedure. The system uses bath sonication and compressed air with a propeller mixer to remove the solvent more

efficiently while mixing the solution. While the solvent is being removed by the system, the jar containing the solution will be placed in a bath sonicator. This extra step will ensure that the CNTs keep their dispersion in the epoxy as the solvent is being removed. A more detailed description on the solvent removal system is described in a section below and a visual image is included in Figure 12.

Once the solvent has been completely removed, the solution will be moved to the vacuum to degas. The resin solution will be kept under bell jar vacuum for 1 hour to ensure excess bubbles created during mixing and any remaining solvent is removed. The hardener can then be added to the resin solution and mixed using a glass stir rod. The resin solution must be cool when the hardener is added in order to keep the epoxy from curing too quickly before all steps are complete. The solution is degassed under vacuum for an additional 20 minutes. This ensures as many bubbles as possible are removed from the epoxy/CNT slurry before it is poured into the cuvettes.

By pouring, the epoxy mixture will be added to cuvette tubes, with care taken not to introduce new bubbles into the solution. Using the vacuum oven, the cuvettes will be degassed for about 30 minutes. The CNTs add more viscosity to the mixture and make it harder to remove all voids in the sample caused by bubbles. Once all bubbles are removed, the samples will be left at room temperature for 48 hours to cure. After the 48-hour cure period, the epoxy samples can be heated at 60C for 1 hour to finish off the first cure step.

A post cure process of the samples is needed to finish the epoxy curing (crosslinking) process and completely solidify the samples. The cuvette container must be removed from the sample before the post cure process to prevent deformation caused by the cuvette material. The only samples not removed from the cuvette during this final cure process are the samples being used for nanoindentation. It is very important to

not allow anything, including fingers or tools, to touch the surface that will be used for nanoindentation. Any change in the surface will affect the results. Therefore, those samples remain in their cuvette covering until they are to be tested. The samples will be moved to the oven and baked for 4 hours at 80 °C. Once cooled down, the samples can be cut to different sizes using a precision sectioning saw; Buehler Isomet 4000. The samples are cut length wise, with the flat sections on the wall of the cuvette being used for the nanoindentation tests and the middle sections for the DMA. Small parts of the samples will be broken to study under SEM. The SEM images are another characterization procedure being used to determine uniform dispersion.

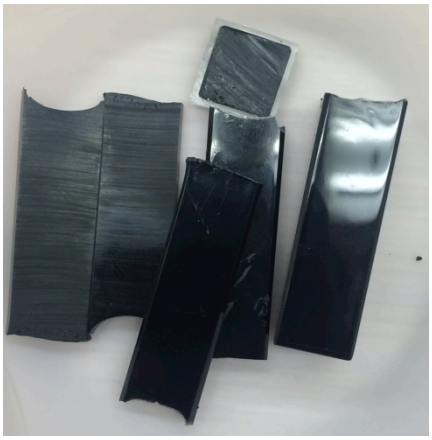

**Figure 9: Image of samples cut from cuvette**

## 2.3 Characterization

### 2.3.1 Raman Spectroscopy

CNT structures were characterized using Raman spectroscopy. Raman spectroscopy can readily determine the crystalline structure of CNTs and the amount of damage that is inflicted upon the CNTs due to ultrasonication by comparing the initial and final CNT structures. It also determines, qualitatively, the amount of functionalization. Pristine CNTs were analyzed using Raman and once the dispersion

process of the CNTs in DCM was completed, CNTs were dried out and analyzed again.

Raman spectrum of carbon nanotubes is unique and exhibits radial breathing mode (RBM), D, and G peaks that are fingerprint of CNTs. The radial breathing mode (RBM) can give a description on the size and type of the CNT being characterized. It is located at the beginning of the spectrum between 75 and 300 $cm^{-1}$. The RBM is known to be inversely proportional to the CNT diameter.[37] The two other modes will be important in this case to observe the effects of the tip sonication and functionalization on the CNT dispersion. The Raman disorder (D) band is around 1330 $cm^{-1}$ and the graphitic (G) band is around 1580 $cm^{-1}$.[37] The most common use of these bands in conjunction with CNT characterization is the G/D ratio. The ratio of intensities between these two bands is indicative of CNT crystallinity. There is also another band that can be seen in some of these spectrographs between the 2500 and 3000 $cm^{-1}$ place. That band is known as the $G^1$ band, is usually appears at about twice the D band wavelength and is a property of graphite and nanotubes. This value is present even for defect free nanotubes. It is important to note that the y-axis units are arbitrary.

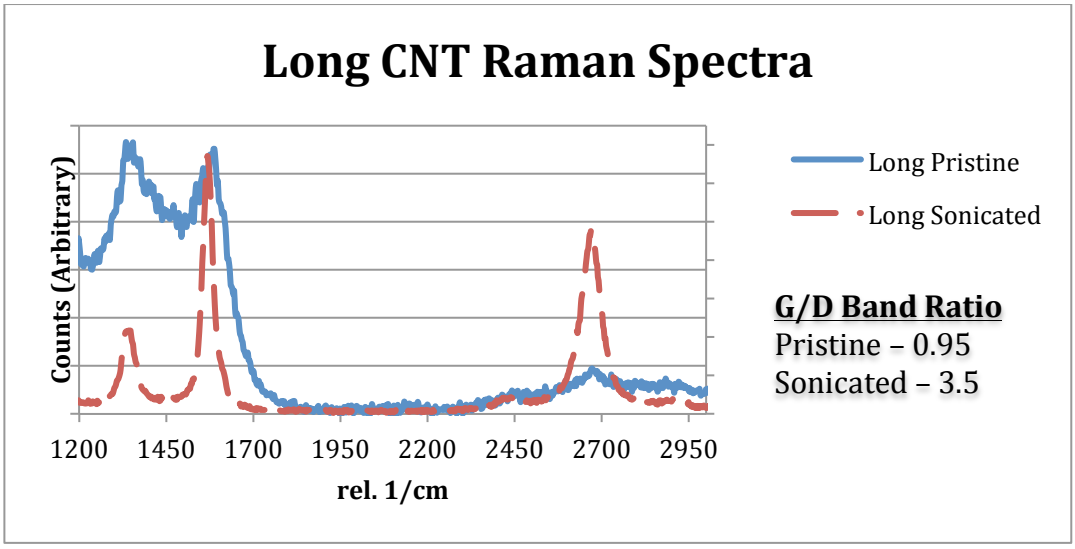


**Figure 10: Raman spectrum of "Long" CNTs**

The spectrograph in Figure 10 is the Raman spectrum of the Long CNTs as received and after dispersion. For the pristine CNT results, the CNTs were mixed, as received, in DCM and a drop was dispersed onto a glass slide for the characterization. The D and G band are very close in intensity and can be indicative of a high defect amount. We believe that these defects are mostly in the form of COOH- functional groups. During the functionalization process, COOH- groups are added to the sidewall and ends of CNTs.

The tip sonication step subjected CNTs to a total energy of 0.5 kJ/mg at 44% amplitude. Such energy level is considered somewhat high and can damage CNTs. It was important that the CNTs in solution were still functional and not too damaged, otherwise the desired properties that were to be achieved through the nanocomposite process would not be met.

The Long CNTs that went through the tip sonication dispersion were also characterized using Raman with the resulting spectrograph compared to the pristine CNTs in Figure 10. The G band is considerably higher in intensity than the D band, as compared to the earlier pristine CNT spectrum. While we expected the

dispersed/centrifuged nanotubes to exhibit a similar or slightly decreased crystallinity ($I_G/I_D$) compared to that of pristine ones, they showed a much higher level of crystallinity ($I_G/I_D$= 3.5). These results prove that the CNTs are crystalline, however, functionalized CNTs were mostly in the form of large aggregates that were separated using the centrifugation step. It is not clear from Raman, how much damage the sonication step has caused.

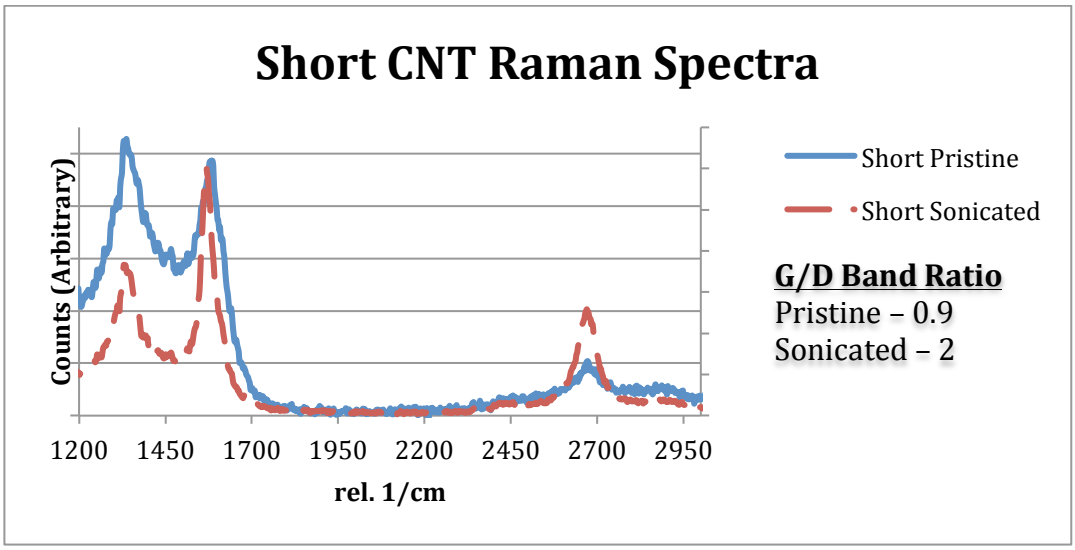


**Figure 11: Raman spectroscopy of "Short" CNTs**

The Raman spectrum of the pristine Short CNTs is shown in Figure 11. A very similar G/D band ratio is observed for the short CNTs. The D and G bands are very close in intensity. The D band intensity is indicative of the COOH- functionalization of the CNTs. Both plots exhibit a 2D band around 2700 $cm^{-1}$. This peak is indicative of CNT dispersion and doping. A better dispersion and less functionalization result in an increase of 2D peak intensity. CNTs exhibited a sharp 2D peak after processing that reveals they are very well dispersed and/or functionalized CNTs have been removed from the solution.

### 2.3.2 Evaporation Device

Evaporation of the solvent from the resin is a vital step in the CNT dispersion process. The solvent must be fully evaporated from the resin for the best epoxy cure and the CNTs must be able to retain a good dispersion in the resin. To that end, an evaporation device was built as shown in Figure 12. The setup involves a heated sonication bath to enhance solvent evaporation, and ultrasonication to prevent agglomeration of the dispersed CNTs as the solvent is being evaporated. The device involved an impeller that was designed to mix the solvent and the resin continuously. A lid, containing two side holes and a hole for the impeller, was used to seal off the jar containing the resin and solvent mixture. One of the holes was used to allow compressed air into the system while the solvent gas was expelled from the second hole. The whole system was designed as a very efficient solvent evaporation setup.

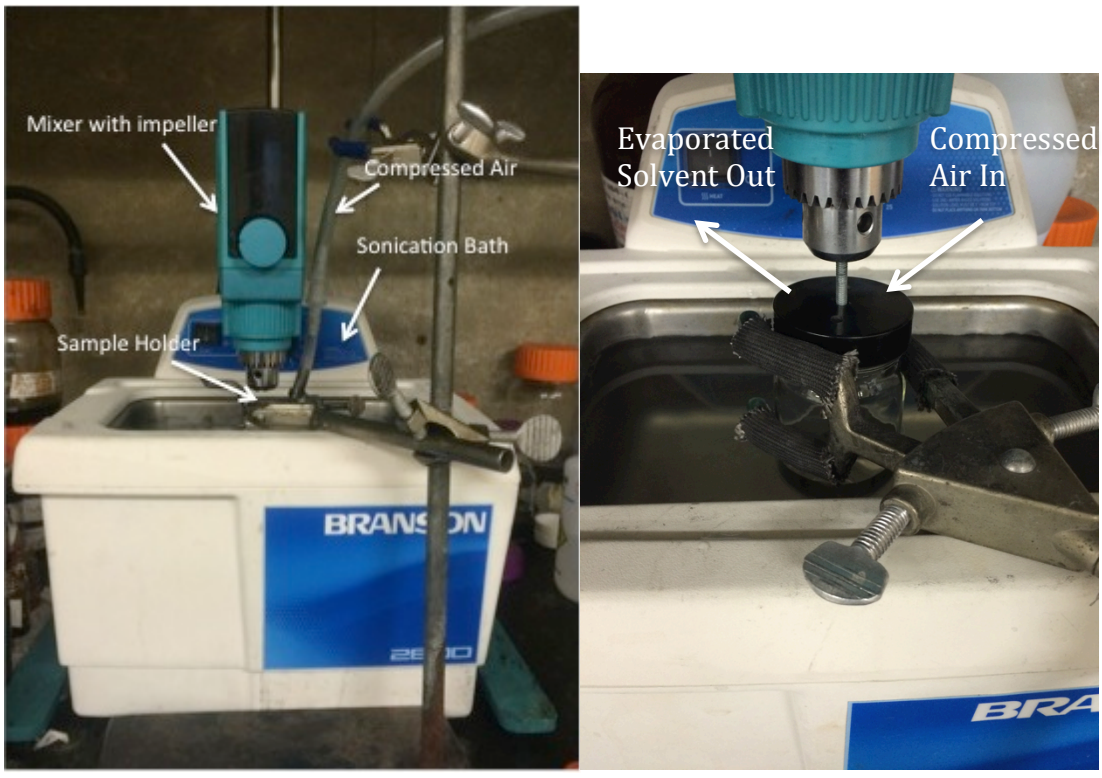


**Figure 12: Evaporation system**

### 2.3.3 Thermogravimetric Analysis & Differential Scanning Calorimetry

Thermogravimetric Analysis (TGA) and Differential Scanning Calorimetry (DSC) were employed to study the effect of solvent and CNT on epoxy curing and verify weight fractions of different phases and impurities in the samples. This test can be performed in both inert or air atmospheres and provides a mass-temperature profile with distinct mass loses for each constituent. For example, when performed in air, solvents are evaporated at their boiling temperature, amorphous carbon burns at ~300 °C, crystalline nanotubes at ~600 °C and the stable residue weight is the metal catalyst. DSC is a programmed measurement of heat absorption/rejection and can give insight into different exo- or endo-thermic processes, e.g., curing, that take place at different temperatures.

As explained earlier, in one of the dispersion methods, CNTs were dispersed in a solution with the aid of surfactants and subsequently centrifuged to collect large aggregates. TGA was first used to determine how much of the surfactant remained in the solution and how much was collected with aggregates during the centrifugation step. Later, a combination of TGA and DSC was used to determine if there was any remaining solvent in the epoxy system, if the epoxy was fully cured before testing, and to verify the CNT or impurity content in samples.

The non-ionic surfactant, Triton X-100 was shown to successfully disperse CNTs in different solvents. A solution of ethanol and Triton X-100 was made with the desired amount of solvent, surfactant, and CNTs. CNTs were mixed with the solvent at a 1:1 mg/ml ratio. The surfactant was mixed at a dispersant to CNT ratio of 2:1. After the centrifugation step, the top portion of the solution, containing the bound, small bundles, and individual nanotubes were collected and the remaining leftover was dried out, at room temperature, and weighed. The weight of agglomerated and

unbound CNTs along with its TGA analysis, determined the amount of well-dispersed CNTs, as well as surfactant content remaining in the master solution.

As shown in Figure 13, almost all of the surfactant remained in the solution and very little was collected at the bottom of the centrifuge vial. This is proven with Thermogravimetric Analysis (TGA) performed on a powdered CNT sample. In this TGA analysis, the sample is heated, in air, at a constant rate of 10°C/min, from room temperature to 850°C, while recording the mass. The Triton X-100 evaporates at a much lower temperature compared to the temperature at which CNT burn.

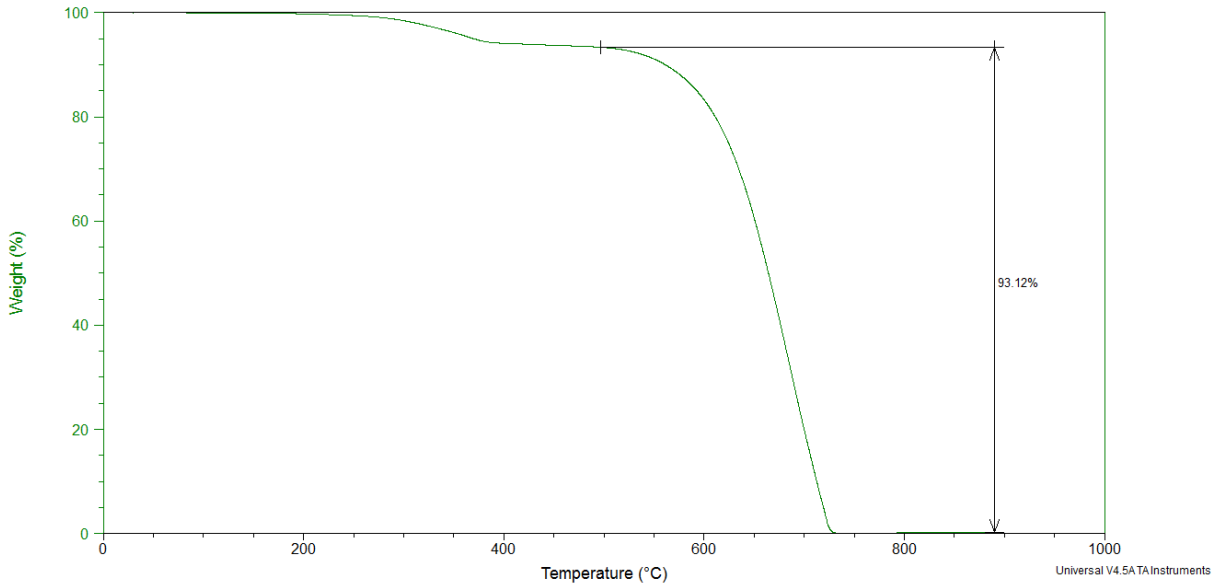


**Figure 13: TGA analysis of CNTs dispersed with Triton X-100**

The TGA data in Figure 13 shows that the CNTs make up about 93wt% of the un-dispersed CNT collection. The same amount of surfactant is added to both solutions, causing a higher concentration of Triton X-100 to remain with a lesser yield of CNTs after the centrifugation step. It was later shown that Triton strongly affects epoxy curing and therefore, the option to disperse CNTs with this surfactant was not further pursued.

DSC was used to determine the cure cycle of the Aeropoxy. It was imperative that the samples were fully cured before final testing. The samples were going to be tested at elevated temperatures and if the full cure was not reached, it would affect the results. TGA was used to verify the weight percent of CNTs in epoxy and whether there is any solvent remained.

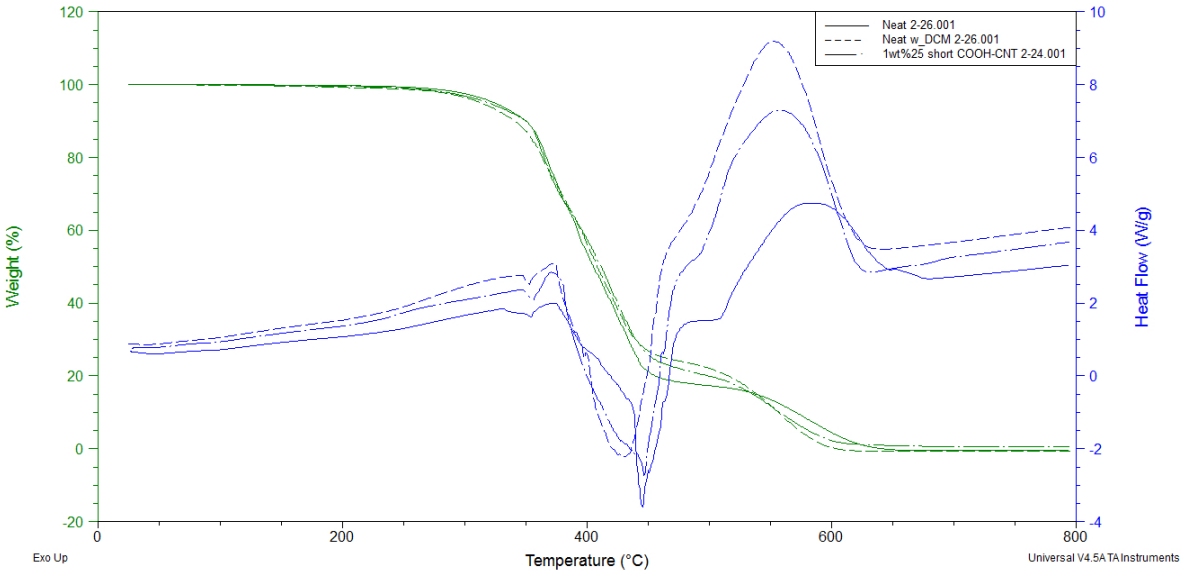


**Figure 14: DSC/TGA of Aeropoxy, Aeropoxy processed with DCM, and Aeropoxy with 1wt% short CNT**

An Aeropoxy sample with DCM evaporated from it was also prepared. The heat flow data in Figure 14 shows a gradual increase from about 100°C to 375°C. This exothermic reaction shows that the epoxy sample is still curing. It was determined from this data that a longer cure was needed. The final samples were then cured for 4 hours instead of the original 2 hours. It is evident, from this DSC curves that both CNTs and DCM affect curing behavior of the epoxy. At about 400°C another reaction is happening in the epoxy mixture. This is the point at which the epoxy is starting to

degrade. The final testing and the glass transition temperature are around 100°C. Therefore, DSC curves at higher temperatures is not discussed here.

It can be also clearly seen that that there is no weight loss around 40°C, i.e., DCM boiling point. More specifically, almost no weight loss occurs before 150°C. The DCM does seem to have an effect on the Aeropoxy and will also be shown with Dynamic Mechanical Analysis.

While the functionalization of the CNTs are predicted to improve bonding of the CNTs with the epoxy matrix, it is unclear if that bonding will cause issues with the final curing of the nanocomposite and resulting mechanical and viscoelastic properties. Some researchers have determined that the functionalization of CNTs does not effect the final curing of the epoxy.

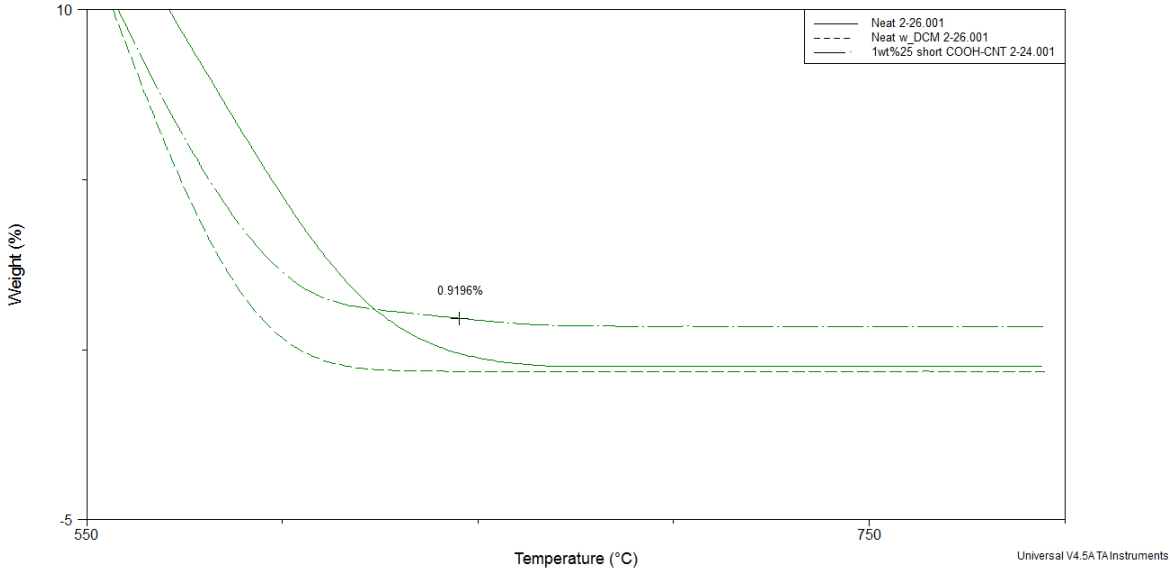


**Figure 15: TGA data of neat Aeropoxy, Aeropoxy with DCM, and 1wt% short CNTs**

Figure 15 is a zoomed in image of the TGA data for the same samples used in Figure 14. CNTs have a much higher temperature of evaporation making TGA a good characterization method to see how much CNT is in the final epoxy samples. The

1wt% sample has a little more than 1wt% CNTs remaining in the sample after the epoxy has been evaporated away.

### 2.3.4 Scanning Electron Microscopy

Scanning Electron Microscopy (SEM) was used to visually determine CNT dispersion within the epoxy. The samples were fractured and coated with a few nanometers thick layer of carbon. CNTs can be seen in the SEM image in Figure 16. CNTs shown in this figure have been pulled out of the epoxy, showing a relatively weak interfacial bonding with the epoxy. Judging by their size, short CNTs are individually dispersed and bundles were not observed.

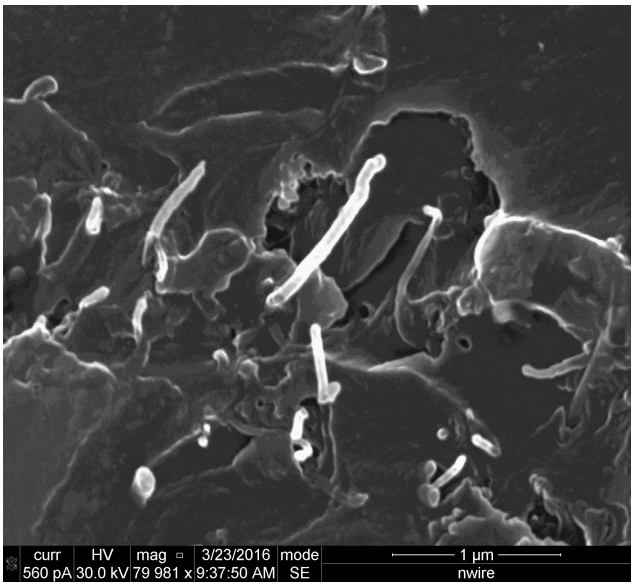


**Figure 16: 1wt% Short sample - SEM image shows close up CNTs in the matrix**

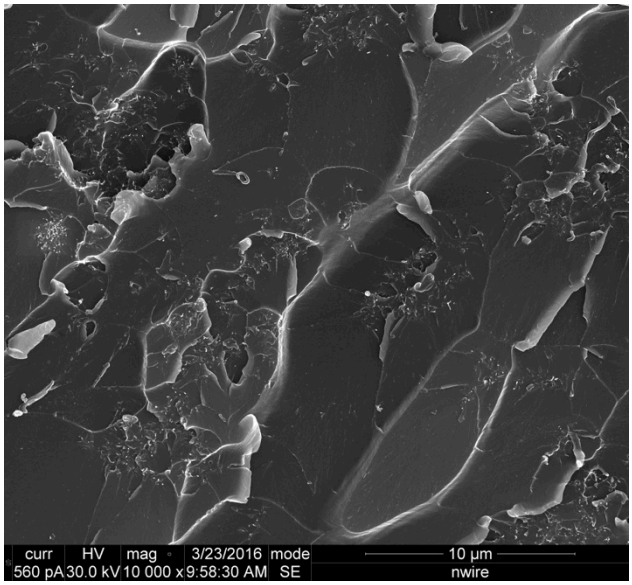


**Figure 17: SEM image of 1wt% long COOH-CNT in epoxy**

The 1wt% samples are shown in Figure 17 and Figure 18. The bright tubular structures are CNT bundles. It does not appear from these images that there are any large aggregates in the samples and the CNTs appear to be well dispersed.

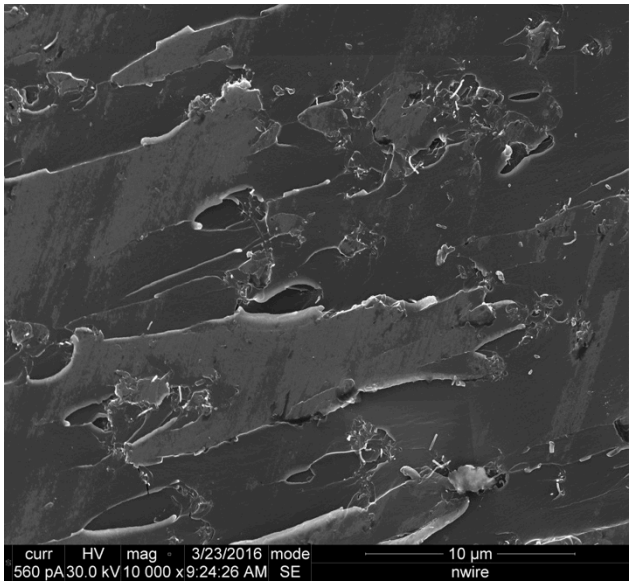


**Figure 18: SEM image of 1wt% short COOH-CNT in epoxy**

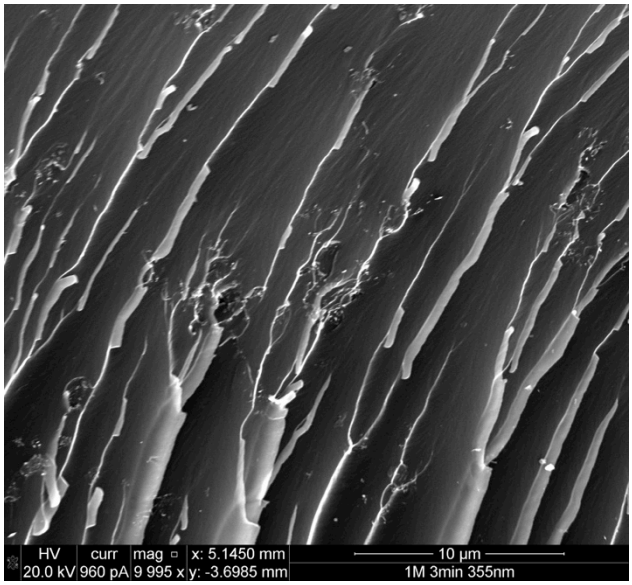


**Figure 19: SEM image of 0.3wt% long COOH-CNTs in epoxy**

The SEM images of the 0.3wt% samples in Figure 19 and Figure 20 also don't show any aggregation of CNTs. The samples appear to have fairly well dispersed CNTs throughout the epoxy.

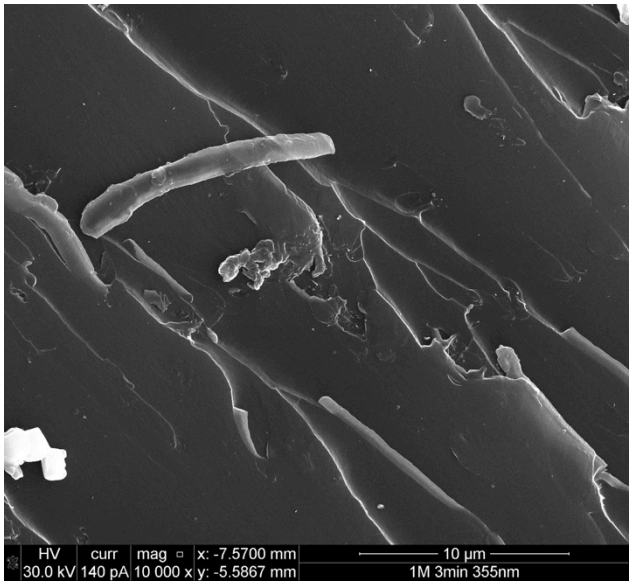


**Figure 20: SEM image of 0.3wt% short COOH-CNTs in epoxy**

# Chapter 3: Dynamic Mechanical Analysis

Dynamic Mechanical Analysis (DMA) tests were performed on a Q800 DMA from TA Instruments. Sample sizes were 25 x 10 x 1.5mm (+/- 0.1 mm). The precision of the Buehler Isomet 4000 saw allowed for samples to meet these very tight requirements. The settings for the DMA testing are represented below, in Table 3.

| Clamp | Three Point Bending |
|---|---|
| Module | Multi-Frequency Strain |
| Method | Temperature Ramp |
| Frequency | 1 Hz |
| Strain | 0.10% |
| Static Force | 0.02 N |
| Force Track | 125% |
| Ramp | 5 °C/min |
| Temperature Range | Room to ~140 °C |

**Table 3: DMA settings used in the measurements**

The settings are for a single frequency and strain rate with a temperature ramping rate of 5 °C/min. A three point bending clamp was used, where a rectangular sample sits on two ends and is subjected to a cyclic force in the middle portion.

Glass transition temperature was extracted from the peak of the tan$\delta$ curve. Multiple pieces were characterized from each sample. Q800 DMA was calibrated before each run.

### 3.1 Solvent Choice

For an effective dispersion in the final nanocomposite, CNTs had to first be dispersed in a solvent, subsequently mixed with the epoxy, followed by solvent removal and final curing. It is important to choose a solvent that not only disperses CNTs well, but also is compatible with the epoxy system and can be readily evaporated (has a low boiling temperature). To test the solvent compatibility, two epoxy samples were made. One was the reference epoxy made per the standard curing protocols. The second sample was the same epoxy resin that was mixed with some solvent. The

solvent was evaporated using the developed setup and cured following the identical procedure as that of the reference sample. The two samples were then tested using DMA to verify solvent-epoxy compatibility.

A few different solvents were tried including tetrahydrofuran (THF), ethanol, acetone, dichloromethane, and a few others. Some were ruled out based on their dispersion abilities in the solution, while others were ruled out based on their degrading effects on the epoxy. Dispersion was tested by visually inspecting the spread of a drop of CNT-solvent solution in a beaker containing pure solvent. Formation of visually identifiable particles was considered a "bad dispersion" while spreading of this dark solution in the same manner as ink would spread in water would be considered a "good dispersion". Stability of CNT-solvent dispersion over night was also inspected. One of the solvents that showed good dispersion and was evaporated from EPON epoxy and tested using DMA was THF. The results of those tests are shown in Figure 21. The storage modulus of the neat EPON sample is much higher, however, the glass transition temperature is lower compared to the sample containing THF in the pre-cured state.

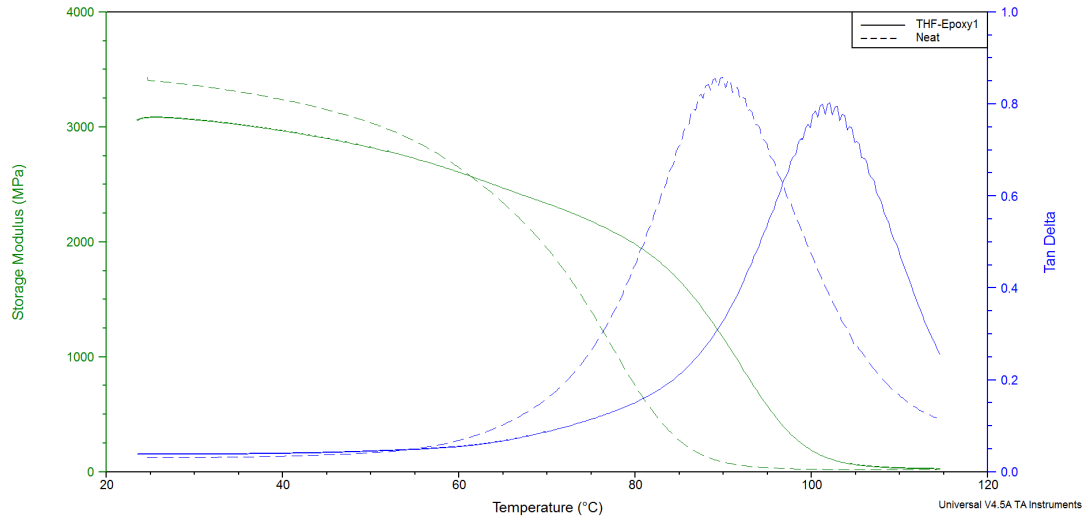


**Figure 21: DMA results of EPON with evaporated THF**

CNT solutions were centrifuged and decanted. The amount of CNTs in the decanted part was used as a quantitative measure for dispersion, i.e., yield. Acetone and ethanol were determined to be the best dispersive solvents for the purpose of testing and had a small effect on DMA properties of the EPON. EPON has a short curing time at room temperature, which proved to be an issue. The process used here needs multiple degassing steps and EPON samples could not be fully degased before curing. An epoxy with a longer gel/cure time was selected. Aeropoxy, as mentioned earlier in Materials, is a medium viscosity resin with a much longer gel/cure time than the EPON. Aeropoxy has been studied by our group and used as matric in carbon fiber, carbon nanotube and other nanoparticle composites.[1, 18, 19, 38-42] Aeropoxy epoxide groups can interact with CNT functional groups to form covalent bonds.

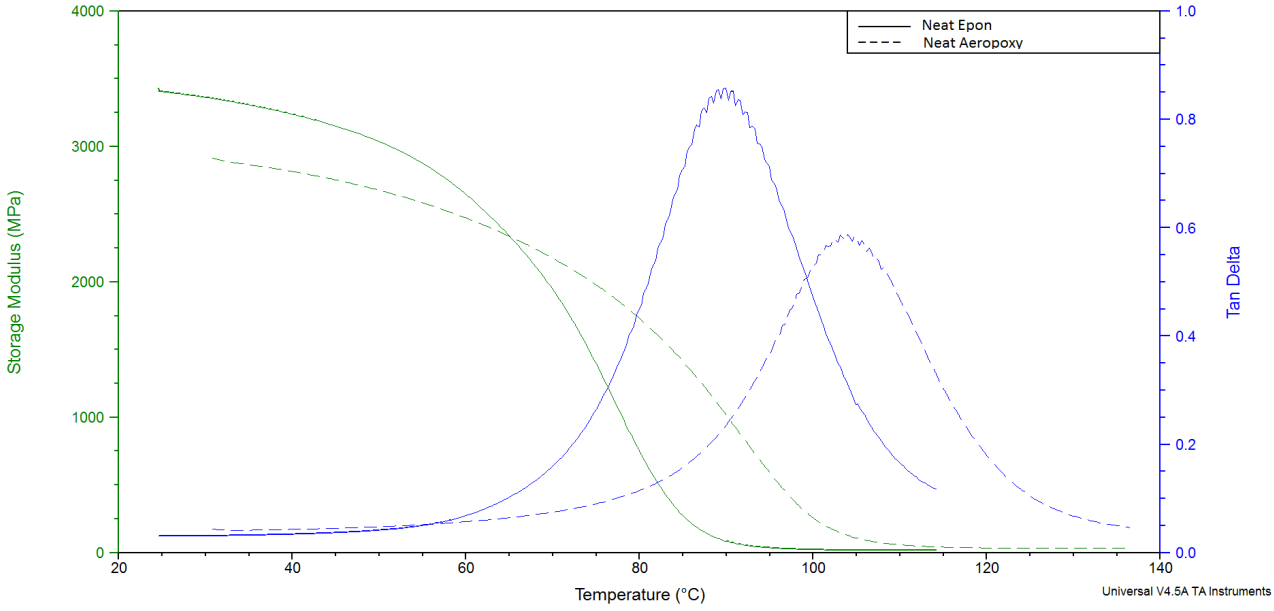


**Figure 22: DMA comparison for EPON and Aeropoxy**

As shown in Figure 22, the two different epoxies have different mechanical properties before any material is added to the matrix. The Aeropoxy has a lower damping than EPON, however, it has a higher glass transition temperature. The next step was to add

the “good” CNT dispersive solvents to the Aeropoxy, evaporate it off and monitor its effect on the DMA properties of Aeropoxy. The DMA comparison is shown in Figure 23.

Acetone and Ethanol with the surfactant, Triton X-100, were shown to be good dispersants. However, once the DCM was tested, the yield ended up being comparable or better than that of acetone or ethanol with surfactant. The comparison in Figure 23 shows that acetone and ethanol/surfactant affect Aeropoxy properties more than DCM or ethanol do. Triton significantly hinders crosslinking polymerization evident by the DMA data.

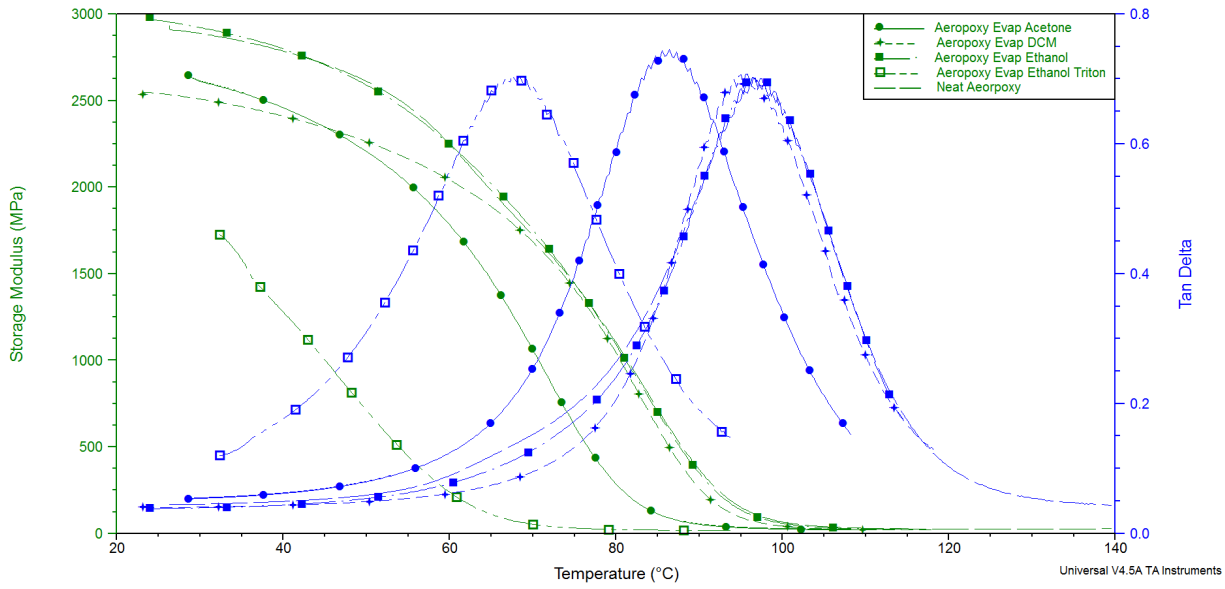


**Figure 23: Solvent in Aeropoxy comparison**

Ethanol without the surfactant had little to no effect on the Aeropoxy, however, the surfactant is needed to achieve a good dispersion of CNTs in solution and a high yield (after centrifugation). DCM also had a relatively small effect on the damping, but a

small decrease in storage modulus was observed. These results are also shown in Figure 24. Based on these results, DCM was chosen as the solvent choice.

All reference epoxy samples were processed with 200 ml of DCM, similar to the amount required for processing of CNT samples.

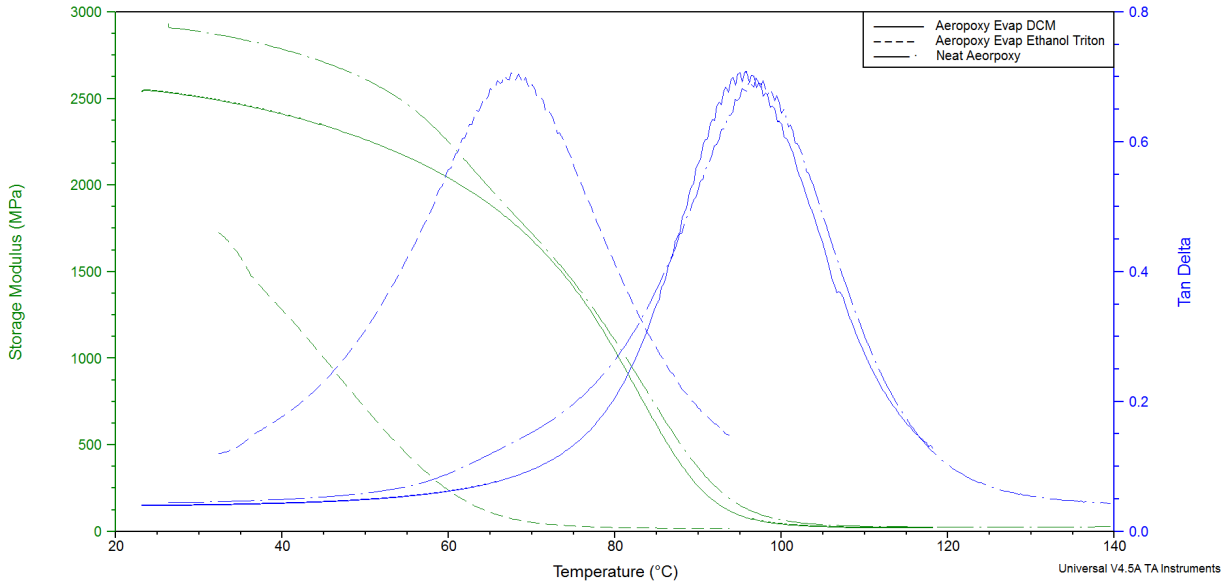


**Figure 24: DMA of Aeropoxy with DCM and Ethanol/Triton evaporated**

### 3.2 Characterization

DMA was performed on different samples containing the different aspect ratio and concentration of CNTs. The DMA overlay for these samples is shown in Figure 25. As expected, DMA responses for all samples are very similar, which is why it is imperative to have very repeatable and consistent samples. Care was taken to keep all the processing and testing conditions identical to prevent any errors.

Multiple samples from each configuration tested. It is important to note that the comparison shown further in the DMA characterization method for different types of

samples is to define a baseline for macro- testing, as well as determine the CNT samples to be compared across the two methods.

Different aspect ration CNTs are supposed to improve the properties differently. In addition to a good dispersion, CNTs should form a strong bond to epoxy for an effective stress transfer.[1] Castillo et al. [43] did a comparison of different types of multiwalled carbon nanotubes and their effects on mechanical properties and glass transition temperatures of nanocomposites. The authors determined that higher aspect ratios of CNTs had a lower percolation threshold. [43] The same trend, up to a certain aspect ratio threshold, was observed by Li et al. [44] Tehrani et al. found that CNTs bond to Aeropoxy (a commercial epoxy) and increase both modulus and hardness, while decrease damping.[1, 18, 38, 41, 45] The increase in linking of the CNTs with the polymer matrix lowers the ability of the epoxy chains to move. [1]

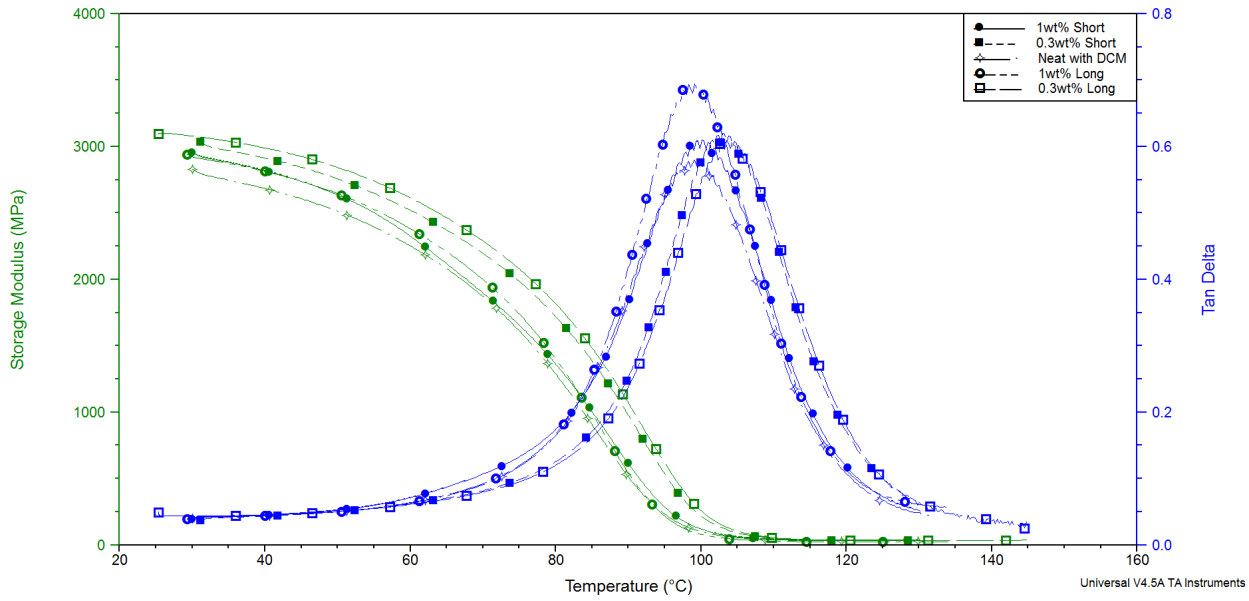


**Figure 25: DMA overlay of all final nanocomposite samples**

The next DMA plot in Figure 26 shows a very close overlay of the results for two different pieces cut from the same sample. Samples were also re-made and

reproducible DMA results were achieved. This proves that the processing was repeatable for multiple pieces and was also an indicator of a good dispersion of the CNTs in the epoxy.

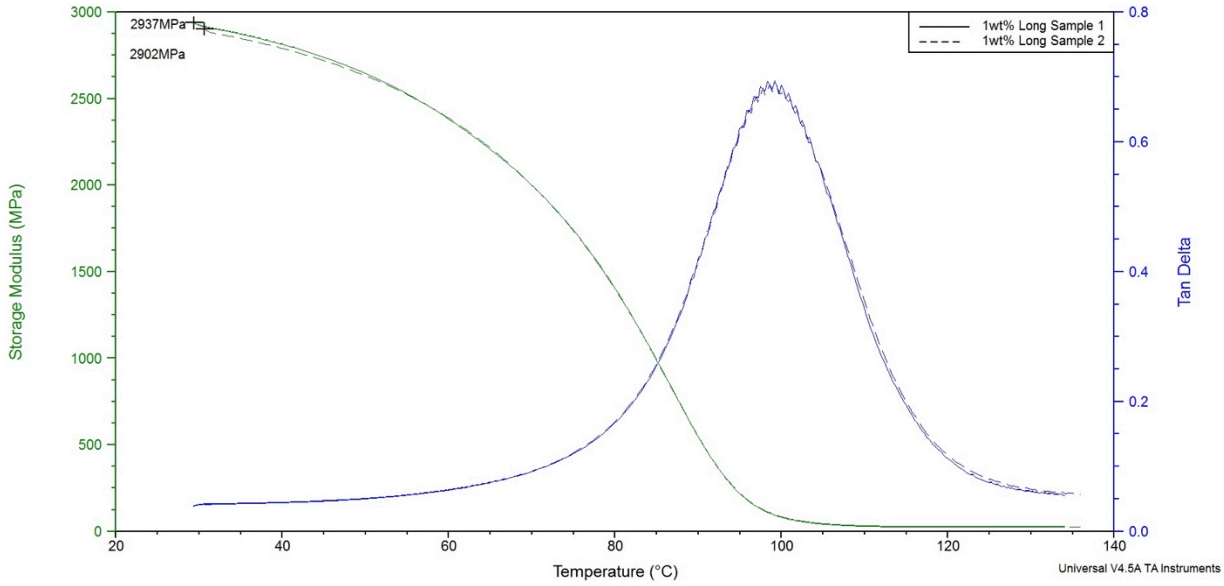


**Figure 26: DMA Results for two pieces of the 1wt% long sample. The comparison shows the uniformity of CNT dispersion in one sample.**

For 0.3 wt% samples, the plots in Figure 27 show an improvement in storage modulus, an increase in glass transition temperature, and an increase in damping. There doesn't seem to be much of a difference between the two CNT types. The long CNTs show slight improvement over the short CNT samples.

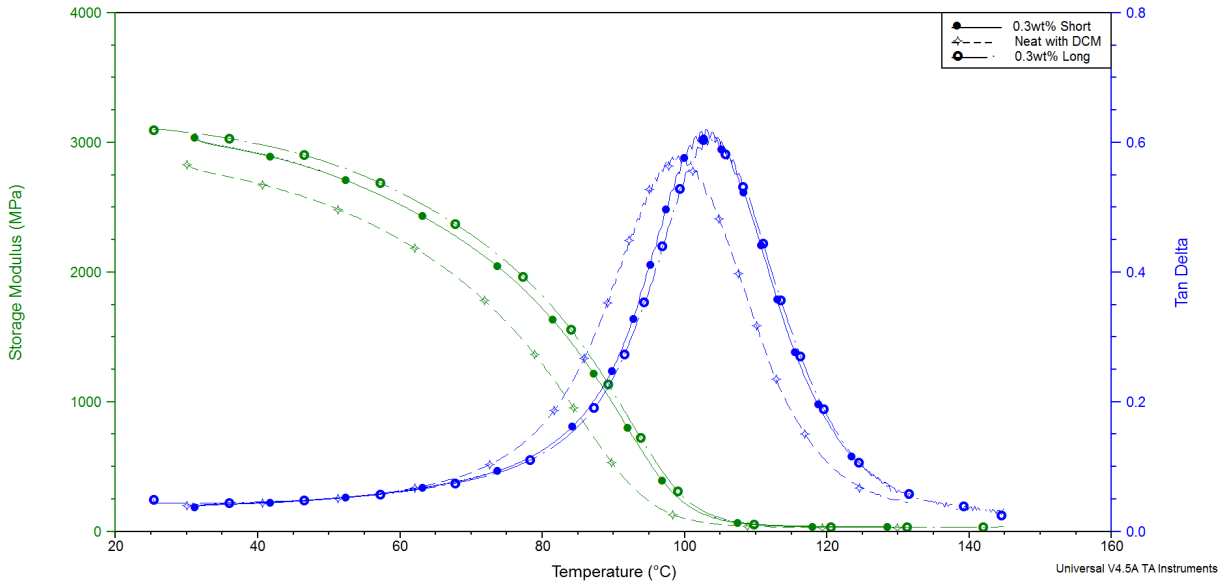


**Figure 27: DMA comparison of 0.3wt% CNTs in Epoxy with different dimensions.**

The same type of comparison can be made for the 1wt% samples, results for which are plotted in Figure 28. There is an improvement in storage modulus and an increased damping in the samples containing 1wt% of CNTs over the neat sample. However, the increase in properties is less than that of the 0.3wt% samples. The long CNT samples also seem to show a slightly higher improvement in damping than the short CNTs.

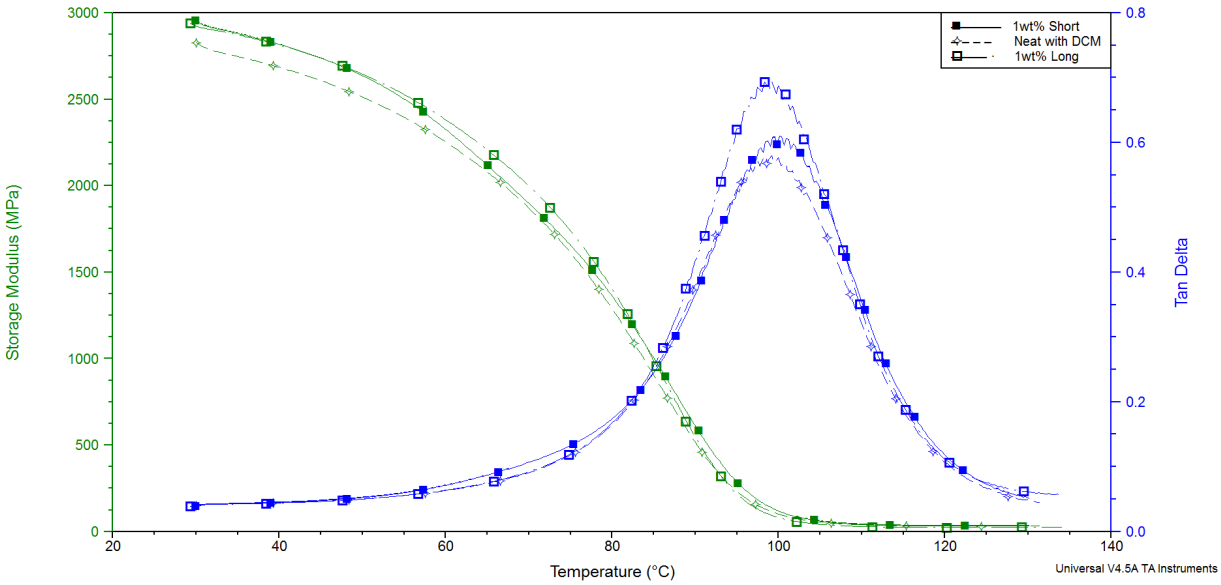


**Figure 28: DMA comparison of 1wt% CNTs in epoxy with different dimensions.**

As mentioned earlier, the 1wt% samples did show improvement in properties, but not as increased of an improvement as the 0.3wt% samples. The next comparison was made between the same CNT types, but at different concentrations. The comparison between the different loadings of the long CNTs are shown in Figure 29 along with the neat epoxy results. The 0.3wt% shows an increase in glass transition temperature as well as an increase in damping compared to the neat epoxy sample. The 1wt% sample shows an even higher increase in damping, but no increase in glass transition temperature. There is also an increase in storage modulus for both CNT samples; however, the 0.3wt% has a greater increase in storage modulus than the 1wt%.

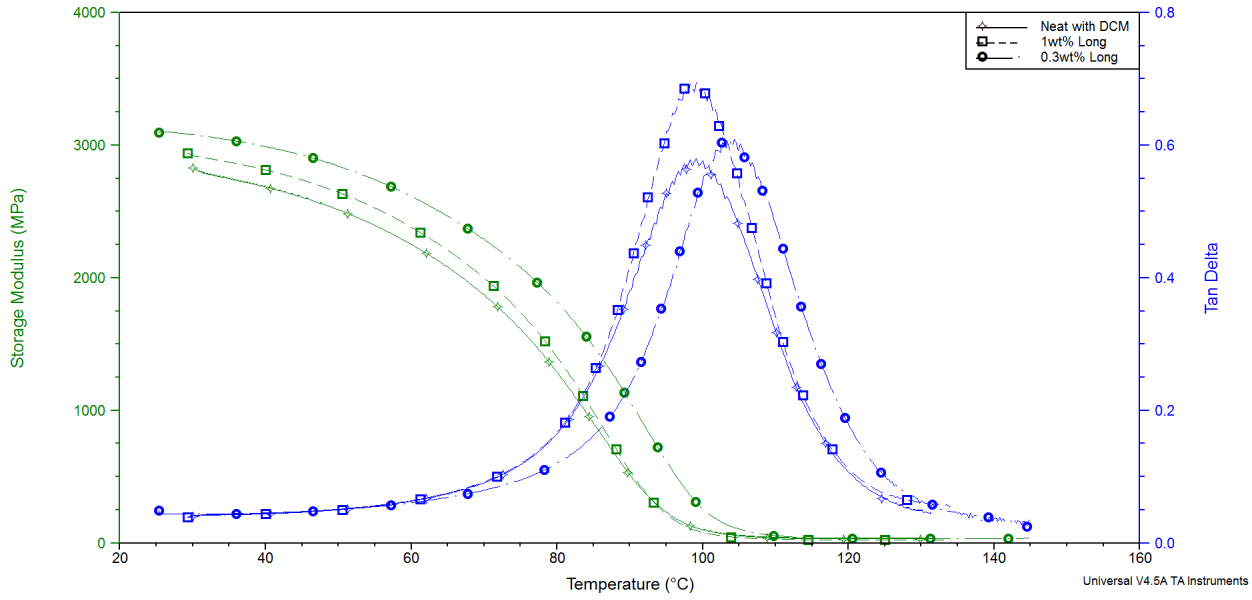


**Figure 29: DMA comparison of long CNTs at different concentrations in epoxy**

The same type of comparison can be made for the short CNTs at different concentrations and is shown in Figure 30. There is a slight increase in damping potential and storage modulus for both concentrations of CNT addition, when compared to the neat epoxy sample. The same trend that was shown in the long samples carries into the short samples. The 0.3wt% samples had an increase in glass transition temperature, while the 1wt% showed a negligible increase in glass transition temperature. The 0.3wt% also showed a higher increase in storage modulus than the 1wt% sample.

The fact that a higher amount of CNTs (1 vs. 0.3) or higher aspect ratio CNTs are not improving the storage modulus as expected is usually attributed to an ineffective stress transfer to CNTs at higher loadings and formation of bundles that can be detrimental to mechanical properties.[1] CNTs can also interfere with polymer curing and effect of improvement and curing cannot be easily distinguished. SEM results show a good dispersion of CNTs in the matrix, however, individual CNTs sticking out

observed SEM micrographs are indicative of a weak binding between polymer and CNTs. Raman results also showed that the processing eliminated some of the functionalized CNTs that could be potentially improving CNT-polymer bonding. This would have been at the expense of having CNT aggregates in the samples that may be detrimental to properties. The second hypothesis (interference with curing) was tested by analyzing the curing behavior of epoxy in the presence of CNTs using the DSC method presented in Chapter 2. DSC results, too, showed some effect on epoxy curing but didn't either prove or disprove this hypothesis. More testing needs to be performed to rule out the effect of CNTs on Aeropoxy curing. For the sake of this work, we are more interested in comparing nanoindentation and DMA results of different samples.

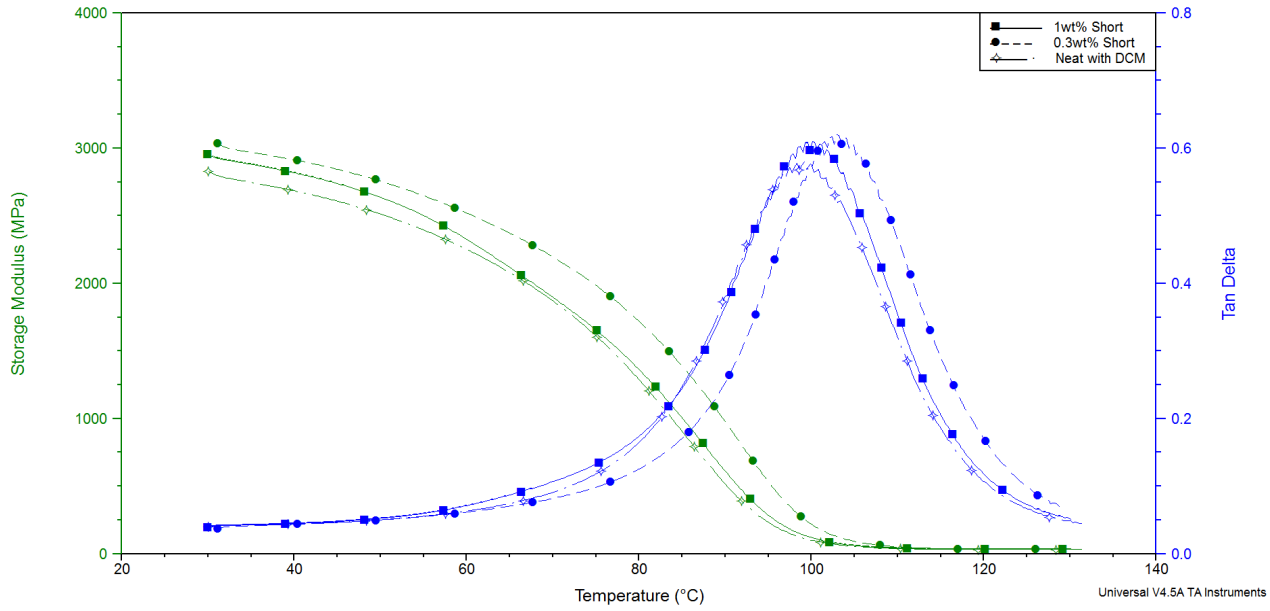


**Figure 30: DMA comparison of the short CNTs at different concentrations in epoxy**

The DMA results of all samples show an interesting trend. All CNT samples have an expected increase in properties. There is an overall increase in storage modulus, damping, and glass transition temperature. The long CNTs had a greater increase in storage modulus and damping, but little increase in glass transition temperature. The

0.3wt% concentrations for both CNT dimensions have a higher storage modulus than the 1wt% samples, but differ on the increase in damping potential. The damping potential is much higher in the 1wt% sample with long CNTs.

# Chapter 4: Instrumented Indentation

Nanoindentation and nanoimpact tests were performed on two different sets of samples: i) the neat Aeropoxy sample (with evaporated DCM) and ii) the Short 0.3wt% sample. It was determined from the DMA testing that the Short 0.3wt% samples had the most desirable increase in properties and dispersion. All tests were performed using a diamond spherical indenter (5 μm in diameter) with the heat shield and samples mounted on the heating stage block.

## 4.1 Nanoindentation

Samples were tested starting at 25°C and then heated up and tested at 90, 95, 100, 105, and 110°C. The 90-110 ranges were to ensure that tests captured the data in the glass transition temperature zone for comparison with DMA values. The 25°C, room temperature, testing was to get a baseline of data for both samples without heating. Our initial experiments involved testing over the 25-120 °C at 10 °C intervals. Sample response was very different than expected due to the prolonged heating periods at each testing temperature. It was therefore decided to only perform the tests between 90-110 °C.

For the elevated temperature tests, the maximum depth was set to go no further than 700 nm. The spherical tip that was employed had a conical shape terminated in a sphere in the last 750 nm of the cone, therefore, going past that depth would get inaccurate results. The 700 nm depth was met, however, during the dwell period at maximum load (100 s), the indenter continued to penetrate deeper, giving a higher maximum depth. To our experience this can slightly affect hardness results and to a greater extent give inaccurate reduced modulus values. For the sake of comparison,

these results are acceptable. The hardness-temperature data from the nanoindentation testing is shown in Figure 31.

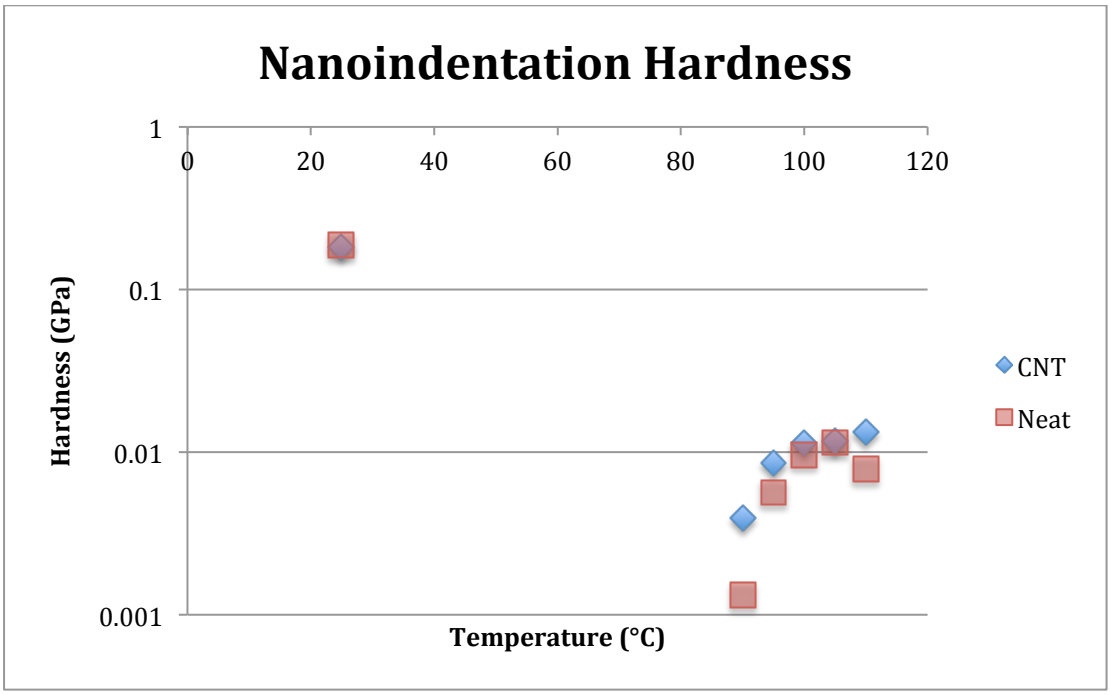


**Figure 31: Hardness data from nanoindentation tests at elevated temperatures for neat and Short 0.3 wt% samples**

There is a trend in the hardness versus temperature data for neat sample, as shown in Figure 31. This could be an indicator of the glass transition temperature. In the DMA testing, it was determined that the $T_g$ of the Neat sample with DCM sample to be 99°C and the $T_g$ of the Short 0.3wt% sample to be 103°C. CNT samples have a higher hardness at all measured temperatures. Hardness values were expected to decrease rapidly in the 90-110 °C range, however both samples harden with increasing the temperature. Neat sample, however show a peak around its $T_g$.

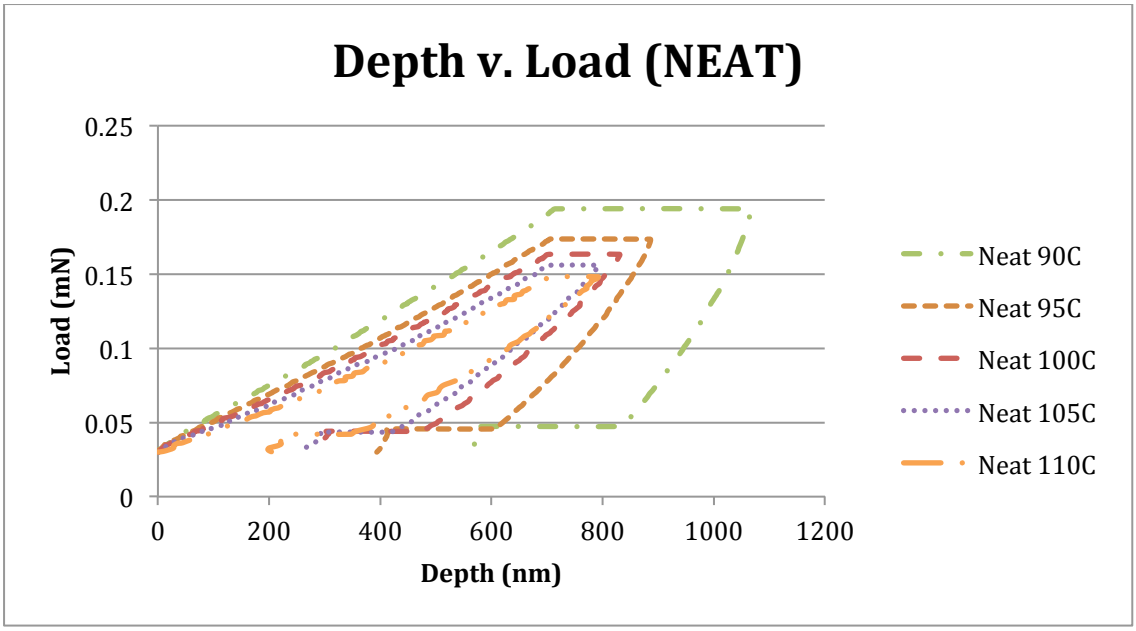


**Figure 32: Depth vs. Load data for the neat with DCM sample**

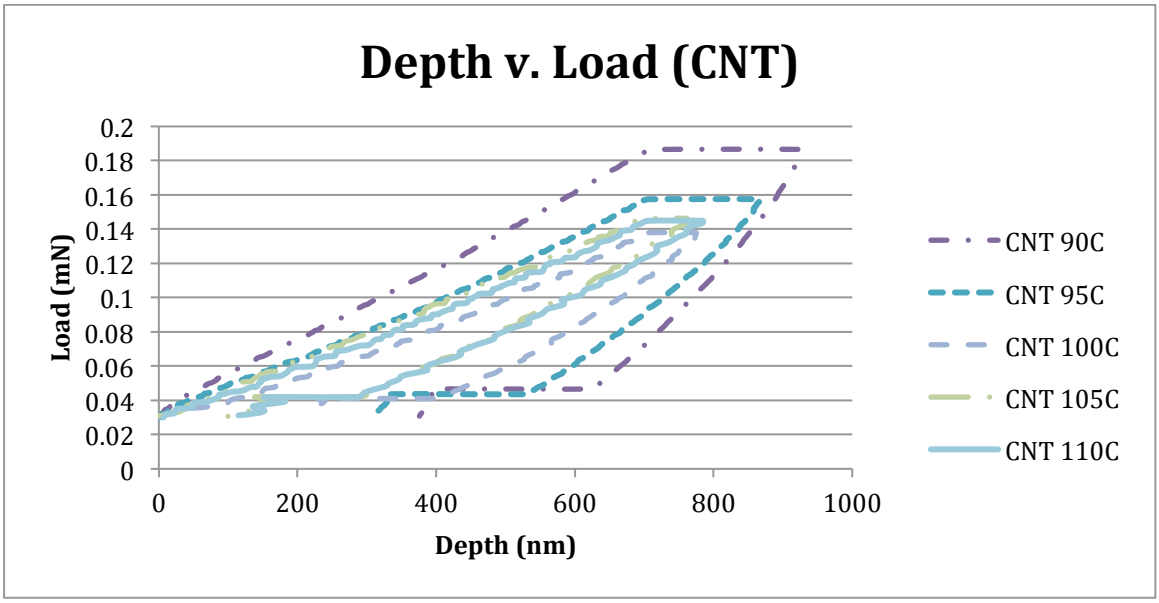


**Figure 33: Depth vs. Load data for short 0.3wt% sample**

The plots shown in Figure 32 and Figure 33 represent the load-depth data for different samples and collected at various temperatures.

The nanoindentation creep data can be used to extract the strain rate sensitivity parameter. The dwell period at maximum hold can be used to show the creep data. An example of the data collected from CNT and Neat samples at 25 °C is shown in Figure

34. The NanoTest software used a best-fit to the creep data and determined the constants A and B, as mentioned earlier in 1.4.2.

The A constant is then used to calculate A/d0 (d0, being the initial depth at maximum load), the strain rate sensitivity parameter. This parameter has been studied as a tool to observe the glass transition temperature [1-3] and is used later as a comparison to tanδ measurements from DMA analysis.

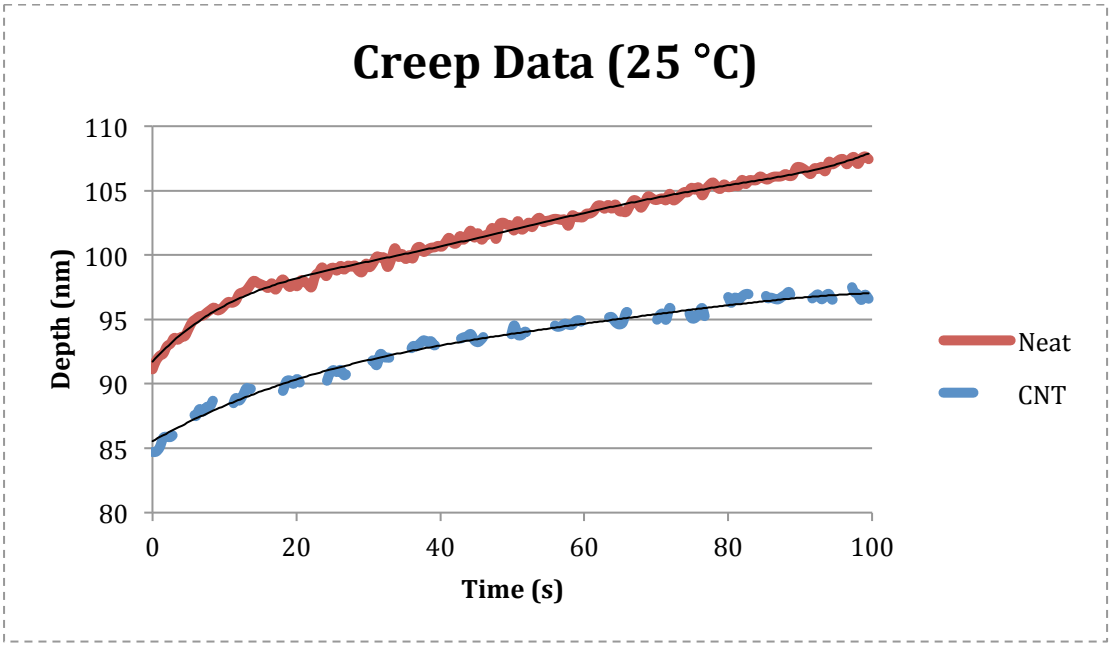


**Figure 34: Creep data with a best fit line shown for CNT and Neat samples at 25C**

### 4.2 Nanoimpact

The Nano Test 600 has the capability to perform nano-impact experiments. Impact tests were used to evaluate the damping ability of a neat Aeropoxy sample and a short 0.3wt% CNT sample. DMA measures the viscoelastic damping while nanoimpact depth-time data contains information on dynamic hardness of the sample, which has contributions form visco-plastic damping. Similar to nanoindentation tests where the unloading response is largely elastic, the bouncing off portion of the nanoimpact test

should be elastic and viscoelastic. It is hypothesized that if this data is analyzed carefully, damping parameters can be extracted. This was not tested in this thesis. The data in Figure 35 shows the data collected from the nano-impact tests that were performed on each sample. Samples were tested at 25°C and 50°C. It can be seen that the neat samples and CNT samples do have minor changes in damping behavior at different temperatures, but it is not visually large enough of a difference to make any conclusions about temperature effects. The difference is, however, large enough between the Neat and CNT samples to come to a conclusion. It appears that the sample with CNTs have a higher damping ability. This is supported by the quicker decay of the oscillations seen in Figure 35 for the CNT samples. Further numerical analysis of this data is required to interpret the data.

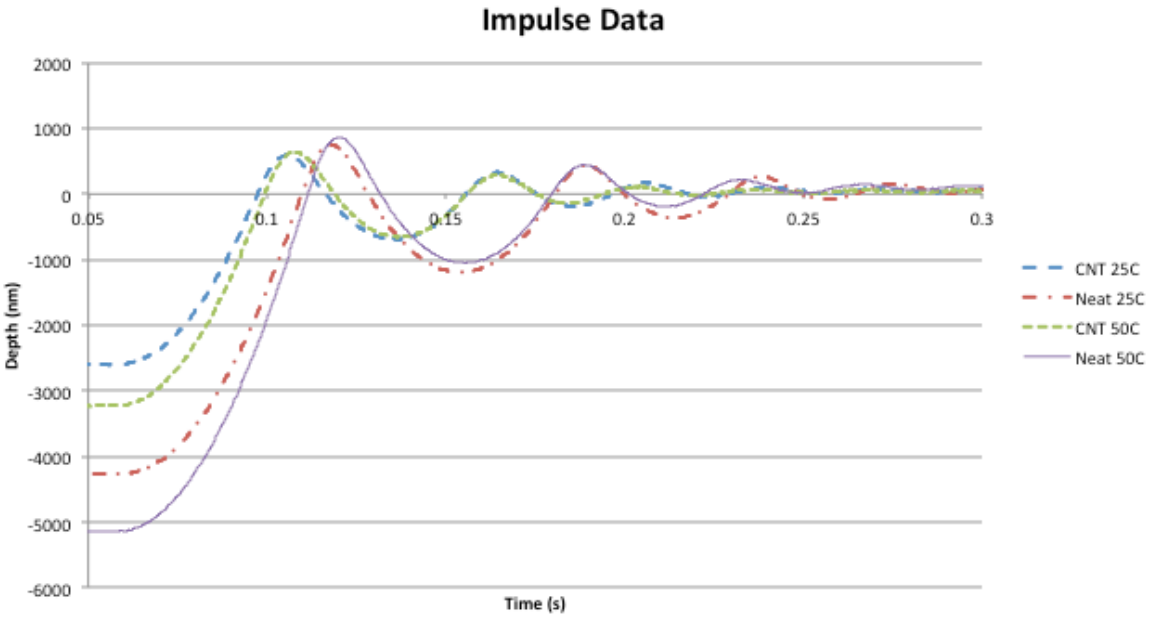


**Figure 35: Representative nanoimpact tests on neat epoxy and CNT nanocomposite**

## Chapter 5: Correlation of DMA and Nanoindentation

Nanoindentation and nano-impact tests were performed at elevated temperatures. Results of these tests are compared to that of DMA tests to see if a correlation can be

made. These data points were compared against each other for both numerical values and thermo-mechanical trends. The data in Table 4 and Figure 36 shows the reduced modulus collected from nanoindentation data. It can be compared to the storage modulus results collected using DMA on the same samples, shown in the plot in Figure 36. The maximum storage modulus results from DMA for the samples were 2.828 GPa and 3.03 GPa for Neat and CNT samples, respectively. In both analysis methods, the samples containing CNTs had a higher room temperature modulus than the samples containing no CNTs. Nanoindentation modulus values are similar to those measured using DMA above $T_g$, however, nanoindentation modulus does not follow the typical decreasing trend with increasing temperature. It can be concluded that surface of sample continues to cure, evident by both increase in hardness and modulus above 90 °C.

Room temperature properties for samples that had been heated up to 110 °C were measured using both nanoindentation and DMA. While post-heat samples showed slight change in DMA measurements, nanoindentation revealed severe degradation of properties on the surface.

| Temperature | Neat - Nanoindentation | Standard Deviation | CNT - Nanoindentation | Standard Deviation |
|---|---|---|---|---|
| 25C | 3.977 GPa | 0.186 | 4.089 GPa | 0.333 |
| 25C – Post Heat | 3.303 GPa | 0.334 | 3.367 GPa | 0.373 |
| 90C | 0.062 GPa | 0.003 | 0.066 GPa | 0.007 |
| 95C | 0.081 GPa | 0.004 | 0.072 GPa | 0.005 |
| 100C | 0.080 GPa | 0.003 | 0.068 GPa | 0.004 |
| 105C | 0.077 GPa | 0.005 | 0.069 GPa | 0.018 |
| 110C | 0.073 GPa | 0.005 | 0.073 GPa | 0.006 |

**Table 4: Reduced Modulus results from nanoindentation data - tabulated**

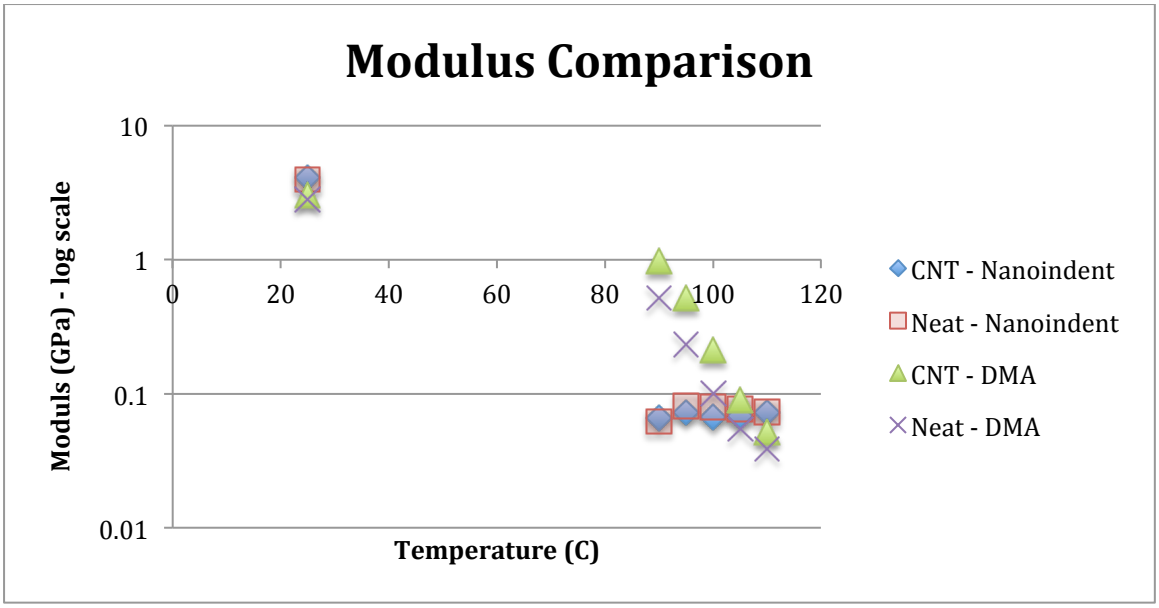


**Figure 36: Nanoindentation Reduced Modulus compared to DMA Storage Modulus as a function of temperature**

Another comparison between the two instruments is the tan$\delta$ data. Using the creep data from nanoindentation and the tan$\delta$ collected from DMA, the correlation mentioned in Gray et al.[3] can be verified. As such, strain rate sensitivity parameter is linearly proportional to tan$\delta$ . Collected data values are shown in Table 5. The highlighted numbers are the maximum from each test. The tan$\delta$ peak is at the glass transition temperature, as shown earlier in DMA data. From the full data set given in DMA, the $T_g$ for the Neat and CNT sample are approximately 99°C and 103°C, respectively. Based on plot of Figure 37, strain rate sensitivity parameter cannot be correlated to damping measured by DMA by any relationship. Moreover, strain rate sensitivity does not follow a similar trend, as the tanδ. We believe this is due to sample surface degradation at elevated temperatures.

| Temperature | Neat - A/d0 | CNT - A/d0 | Neat - tan delta | CNT - tan delta |
|---|---|---|---|---|
| 25 C | 0.0787 | 0.0807 | 0.0406 | 0.0373 |
| 90 C | 0.1371 | 0.0773 | 0.3862 | 0.2587 |
| 95 C | 0.0592 | 0.0451 | 0.5238 | 0.4115 |
| 100 C | 0.0376 | 0.0322 | 0.5649 | 0.5735 |
| 105 C | 0.0339 | 0.0299 | 0.4752 | 0.5893 |
| 110 C | 0.0414 | 0.0246 | 0.3176 | 0.4592 |
| 25 C - Post Heat | 0.0585 | 0.0804 | --------- | ---------- |

**Table 5: A/d(0) from nanoindentation and tanδ data from DMA**

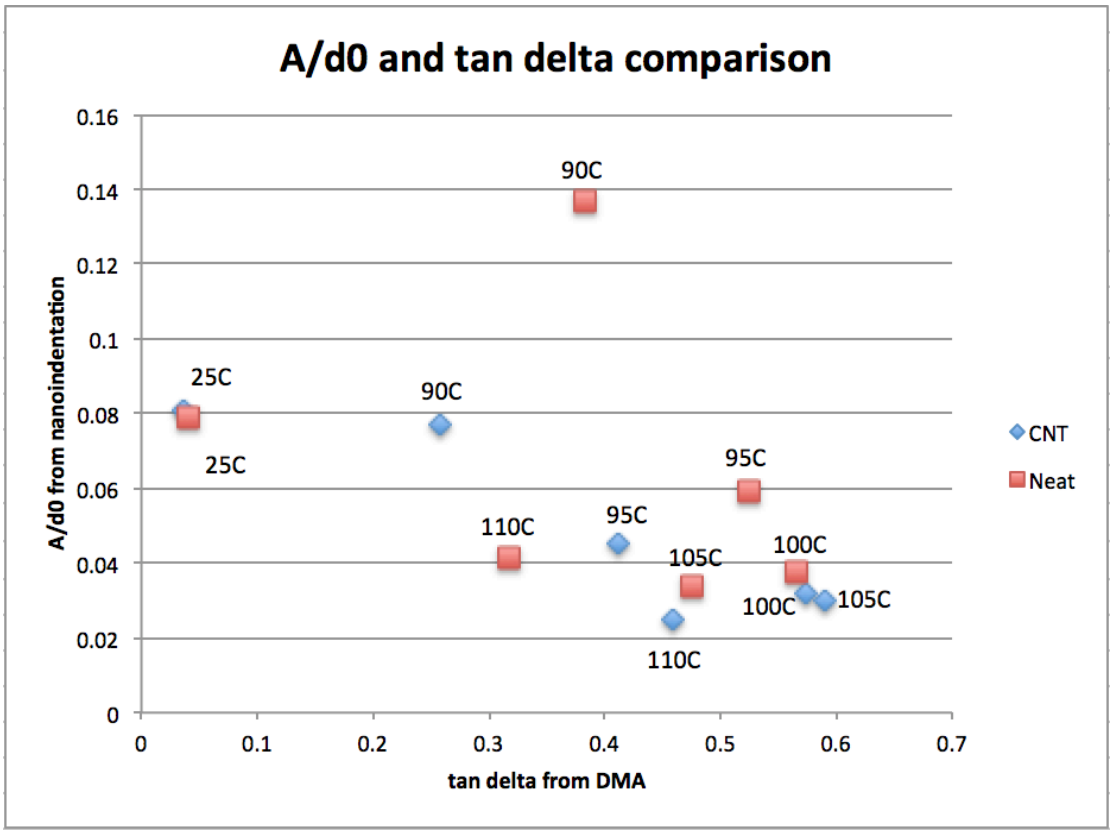


**Figure 37: Graphic representation of A/d0 and tan delta comparison**

Tanδ is not only an indicator of $T_g$, but also measures the damping ability of a material. From the DMA data, samples containing CNTs had a higher viscoelastic damping ability, compared to the sample without CNTs. This trend is also proven to be true by the nano-impact testing. The oscillations show a better viscoplastic

damping ability in the sample containing CNTs, when compared to the neat Aeropoxy sample.

The data from DMA and nanoindentation can be compared and corroborated in some of the mechanical and viscoelastic properties. More samples could have been tested and a greater range of temperatures other testing parameters performed. Most importantly, samples have to be tested in an inert atmosphere where their surfaces are protected from degradation by oxidation.

## Chapter 6: Future Work

The type of CNTs, concentrations, and method of dispersion all played a role in the mechanical and viscoelastic properties of the samples. There are many other processing parameters that need to be optimized for an effective CNT-epoxy integration. It would be interesting to elucidate the role of processing on elimination of functionalized CNTs (confirmed by Raman).

All final samples were made within the span of a week and all from two master batches of solution. This insured that all samples were prepared under the best identical lab conditions possible. It will be worthwhile to systematically investigate the effect of both intensity/duration of air exposure, temperature and humidity during processing and after samples are cured, on the core and surface properties of the nanocomposites. For example, preliminary testing determined that any moisture would significantly affect the dispersion of CNTs. If moisture plays that big of a role, it would be interesting to see what temperature does for different polymer and solvent combinations. We also observed severe surface degradations due to elevated temperatures, but to a much lower degree for samples tested using DMA. Such degradations need to be understood and minimized in order for nanoindentation results to be consistent with the bulk properties. One possible approach would be to perform nanoindentation in an enclosure filled with an inert gas.

Other parameters have been shown to make a difference in nanocomposite properties. These include epoxy types, solvents, surfactants, and order of mixing. Our understanding is that developing standardized methods to prepare nanocomposite samples will be the corner stone to much of the research being done pertaining to these types of nanocomposites.

Finally, further characterization of CNT morphology and structure would be beneficial to learn more about these composites. In this study, only thermo-mechanical and calorimetric studies were conducted, but electrical properties are also important to gain an understanding of dispersion and connectivity of CNTs in the matrix.

Overall, more experiments and simulations need to be performed to fully understand nanocomposites and correlate their nano- to macro- mechanical properties.

References

1. Tehrani, M., M. Safdari, and M.S. Al-Haik, *Nanocharacterization of creep behavior of multiwall carbon nanotubes/epoxy nanocomposite.* International Journal of Plasticity, 2011. **27**(6): p. 887-901.

2. Beake, B.D., et al., *Nanoindentation creep and glass transition temperatures in polymers.* Polymer International, 2007. **56**(6): p. 773-778.

3. Gray, A., D. Orecchia, and B.D. Beake, *Nanoindentation of Advanced Polymers Under Non-Ambient Conditions: Creep Modelling and Tan Delta.* Journal of Nanoscience and Nanotechnology, 2009. **9**(7): p. 4514-4519.

4. Iijima, S., *Helical Microtubules of Graphitic Carbon.* Letters to Nature, 1991. **354**: p. 56-58.

5. Breuer, O. and U. Sundararaj, *Big Returns From Small Fibers: A Review on Polymer/Carbon Nanotube Composites.* Polymer Composites, 2004. **25**(6): p. 630-645.

6. Andrews, R., et al., *Purification and Structural Annealing of Multiwalled Carbon Nanotubes at Graphetization Temperatures.* Carbon, 2001. **39**: p. 1681-1687.

7. Rana, S., R. Alagirusamy, and M. Joshi, *A Review on Carbon Epoxy Nanocomposites.* Journal of Reinforced Plastics and Composites, 2009. **28**(4): p. 461-487.

8. Vaisman, L., H.D. Wagner, and G. Marom, *The role of surfactants in dispersion of carbon nanotubes.* Advances in Colloid and Interface Science, 2006: p. 37-46.

9. Xin, F. and L. Li, *Effect of Triton X-100 on MWCNT/PP composites.* Journal of Thermoplastic Composite Materials, 2013. **26**(2): p. 227-242.

10. Dehghan, M., et al., *Surfactant-Assisted Dispersion of MWCNTs in Epoxy Resin Used in CFRP Strengthening Systems.* Journal of Adhesion, 2015. **91**(6): p. 461-480.

11. Sahoo, N.G., et al., *Polymer nanocomposites based on functionalized carbon nanotubes.* Progress in Polymer Science, 2010. **35**: p. 837-867.

12. Hussain, F., et al., *Review article: Polymer-matrix nanocomposites, processing, manufacturing, and application: An overview.* Journal of Composite Materials, 2006. **40**(17): p. 1511-1575.

13. Moniruzzaman, M. and K.I. Winey, *Polymer nanocomposites containing carbon nanotubes.* Macromolecules, 2006. **39**(16): p. 5194-5205.

14. Sahoo, N.G., et al., *Polymer nanocomposites based on functionalized carbon nanotubes.* Progress in Polymer Science, 2010. **35**(7): p. 837-867.

15. *QSonica Sonicator Brochure*. 2011, Cole Palmer.

16. Montazeri, A., et al., *The effect of sonication time and dispersing medium on the mechanical properties of multiwalled carbon nanotube (MWCNT)/ Epoxy composite.* International Journal of Polymer Analysis and Characterization, 2011. **16**: p. 465-476.

17. Gibson, R.F., *A review of recent research on nanoindentation of polymer composites and their constituents.* Composites Science and Technology, 2014. **105**: p. 51-65.

18. Tehrani, M., et al., *Mechanical characterization and impact damage assessment of a woven carbon fiber reinforced carbon nanotube-epoxy composite.* Composites Science and Technology, 2013. **75**: p. 42-48.

19. Tehrani, M., et al., *Hybrid carbon fiber/carbon nanotube composites for structural damping applications.* Nanotechnology, 2013. **24**(15).

20. Pizzutto, C.E., et al., *Study of Epoxy/CNT Nanocomposites Prepared Via Dispersion in the Hardener.* Materials Research-Ibero-American Journal of Materials, 2011. **14**(2): p. 256-263.

21. Yoonessi, M., et al., *Carbon Nanotube Epoxy Nanocomposites: The Effects of Interfacial Modifications on the Dynamic Mechanical Properties of the Nanocomposites.* Acs Applied Materials & Interfaces, 2014. **6**(19): p. 16621-16630.

22. Zhu, J., et al., *Improving the dispersion and integration of single-walled carbon nanotubes in epoxy composites through functionalization.* Nano Letters, 2003. **3**(8): p. 1107-1113.

23. Abdalla, M., et al., *The effect of interfacial chemistry on molecular mobility and morphology of multiwalled carbon nanotubes epoxy nanocomposite.* Polymer, 2007. **48**(19): p. 5662-5670.

24. Abdullah, M.P. and S.A. Zulkepli, *The Functionalization and Characterization of Multi-walled Carbon Nanotubes (MWCNTs)*. 2015 Ukm Fst Postgraduate Colloquium, 2015. **1678**.

25. Oliver, W.C. and G.M. Pharr, *An Improved Technique for Determining Hardness and Elastic-Modulus Using Load and Displacement Sensing Indentation Experiments.* Journal of Materials Research, 1992. **7**(6): p. 1564-1583.

26. Oliver, W.C. and G.M. Pharr, *Measurement of hardness and elastic modulus by instrumented indentation: Advances in understanding and refinements to methodology.* Journal of Materials Research, 2004. **19**(1): p. 3-20.

27. Rohini, R. and S. Bose, *Tailored interface and enhanced elastic modulus in epoxy-based composites in presence of branched poly(ethyleneimine) grafted multiwall carbon nanotubes.* Physical Chemistry Chemical Physics, 2015. **17**(12): p. 7907-7913.

28. Choudhary, N., et al., *NiTi/Pb(Zr0.52Ti0.48)O-3 thin film heterostructures for vibration damping in MEMS.* Sensors and Actuators a-Physical, 2013. **193**: p. 30-34.

29. Riester, L., M.K. Ferber, and K. Breder, *Elastic modulus calculations from load/displacement curves using spherical and pointed indenters.* Nondestructive Evaluation of Ceramics, 1998. **89**: p. 337-344.

30. Odegard, G.M., T. Gates, and H.M. Herring, *Characterization of viscoelastic properties of polymeric materials through nanoindentation.* Experimental Mechanics, 2005. **45**(2): p. 130-136.

31. Tehrani, M., *Effect of Moderate Magnetic Annealing on the Microstructure and Mechanical Behavior of a Structural Epoxy*, in *Mechanical Engineering*. 2009, The University of New Mexico.

32. Beake, B.D., V.M. Vishnyakov, and J.S. Colligon, *Nano-impact testing of TiFeN and TiFeMoN films for dynamic toughness evaluation.* Journal of Physics D-Applied Physics, 2011. **44**(8).

33. *How to select the correct indenter tip*. Support Note 2009.

34. Tehrani, M., *Next Generation Multifunctional Composites for Impact, Vibration and Electromagnetic Radiation Hazard Mitigation*, in *Engineering Mechanics*. 2012, Virginia Polytechnic Institute and State University

35. Herbert, E.G., W.C. Oliver, and G.M. Pharr, *Nanoindentation and the dynamic characterization of viscoelastic solids.* Journal of Physics D-Applied Physics, 2008. **41**.

36. Ayatollahi, M.R., et al., *Effect of multi-walled carbon nanotube aspect ratio on mechanical and electrical properties of epoxy-based nanocomposites.* Polymer Testing, 2011. **30**: p. 548-556.

37. *Characterization of Carbon Nanotubes (CNTs) with Raman Spectroscopy*. DeltaNu, Inc.: http://www.deltanu.com.

38. Tehrani, M., et al., *Synthesis of WS2 nanostructures from the reaction of WO3 with CS2 and mechanical characterization of WS2 nanotube composites.* Nanotechnology, 2011. **22**(28).

39. Tehrani, M., et al., *Effect of Moderate Magnetic Annealing on the Microstructure, Quasi-Static, and Viscoelastic Mechanical Behavior of a Structural Epoxy.* Journal of Engineering Materials and Technology-Transactions of the Asme, 2012. **134**(1).

40. Tehrani, M., et al., *Using Multiscale Carbon Fiber/Carbon Nanotubes Composites for Damping Applications.* Proceedings of the Asme Conference on Smart Materials, Adaptive Structures and Intelligent Systems (Smasis 2011), Vol 1, 2012: p. 129-133.

41. Tehrani, M., et al., *Impact and Quasi-Static Mechanical Properties of a Carbon Fiber Reinforced Carbon Nanotube/Epdxy.* International Mechanical Engineering Congress and Exposition - 2012, Vol 3, Pts a-C: Design, Materials, and Manufacturing, 2013: p. 1315-1320.

42. Tehrani, M., et al., *Mechanical Characterization of a Hybrid Carbon Nanotube/Carbon Fiber Reinforced Composite.* Proceedings of the Asme International Mechanical Engineering Congress and Exposition, 2013, Vol 9, 2014.

43. Castillo, F.Y., et al., *Electrical, mechanical, and glass transition behavior of polycarbonate-based nanocomposites with different multi-walled carbon nanotubes.* Polymer, 2011. **52**(17): p. 3835-3845.

44. Li, J., et al., *Correlations between Percolation Threshold, Dispersion State,and Aspect Ratio of Carbon Nanotubes.* Advanced Funtional Materials, 2007. **17**: p. 3207-3215.

45. Boroujeni, A.Y., et al., *Hybrid carbon nanotube-carbon fiber composites with improved in-plane mechanical properties.* Composites Part B-Engineering, 2014. **66**: p. 475-483.

45. Moniruzzaman, M. and K.I. Winey, *Polymer nanocomposites containing carbon nanotubes.* Macromolecules, 2006. **39**(16): p. 5194-5205.

46. Dai, H.J., *Carbon nanotubes: Synthesis, integration, and properties.* Accounts of Chemical Research, 2002. **35**(12): p. 1035-1044.

47. Hussain, F., et al., *Review article: Polymer-matrix nanocomposites, processing, manufacturing, and application: An overview.* Journal of Composite Materials, 2006. **40**(17): p. 1511-1575.

48. Montazeri, A., et al., *The Effect of Curing Cycle on the Mechanical Properties of Mwnt/Epoxy Nanocomposite.* International Journal of Polymer Analysis and Characterization, 2010. **15**(3): p. 182-190.

49. Guadagno, L., et al., *Effect of functionalization on the thermo-mechanical and electrical behavior of multi-wall carbon nanotube/epoxy composites.* Carbon, 2011. **49**: p. 1919-1930.

50. Abdalla, M., et al., *Cure behavior of epoxy/MWCNT nanocomposites: The effect of nanotube surface modification.* Polymer, 2008. **49**: p. 3310-3317.

51. Aboubakr, S.H., U.F. Kandil, and M.R. Taha, *Creep of epoxy-clay nanocomposite adhesive at the FRP interface: A multi-scale investigation.* International Journal of Adhesion & Adhesives, 2014. **54**.

52. Ma, P.-C., et al., *Dispersion, interfacial interaction and re-agglomeration of functionalized carbon nanotubes in epoxy composites.* Carbon, 2010. **48**: p. 1824-1834.

53. Schlagenhauf, L., et al., *Decomposition and particle reease of a carbon nanotube/epoxy nanocomposite at elevated temperatures.* Journal of Nanoparticle Research, 2015. **17**(440).

54. Evseeva, L.E. and S.A. Tanaeva, *Influence of the concentration of carbon nanotubes (CNT) on the thermophysical properties of epoxy/CNT nanocomposites at low temperatures.* Mechanics of Composite Materials, 2008. **44**(5).

55. Park, J.G., et al., *Thermal conductivity of MWCNT/epoxy composites: The effects of length, alignment and functionalization.* Carbon, 2012. **50**: p. 2083-2090.

56. Guadagno, L., et al., *Mechanical and barrier properties of epoxy resin filled with multi-walled carbon nanotubes.* Carbon, 2009. **47**: p. 2419-2430.

57. Lau, K.T., et al., *Thermal and mechanical properties of single-walled carbon nanotube bundle-reinforced epoxy nanocomposites: the role of solvent for nanotube dispersion.* Composites Science and Technology, 2005. **65**(5): p. 719-725.

58. Pantano, A. (2012). *Carbon nanotube based composites: Processing, properties, modeling and application.* Shawbury, Shrewsbury, Shropshire: Smithers Rapra. http://public.eblib.com/choice/publicfullrecord.aspx?p=1114560

59. Advani, S. G. (2007). *Processing and properties of nanocomposites.* Singapore: World Scientific Pub.. http://www.books24x7.com/marc.asp?bookid=25715